

Zeolites and Associated Authigenic Silicate Minerals in Tuffaceous Rocks of the Big Sandy Formation, Mohave County, Arizona

By RICHARD A. SHEPPARD and ARTHUR J. GUDE 3d

GEOLOGICAL SURVEY PROFESSIONAL PAPER 830

Physical properties, chemistry, and origin of silicate minerals formed in tuffaceous rocks of a Pliocene lacustrine deposit



UNITED STATES DEPARTMENT OF THE INTERIOR

ROGERS C. B. MORTON, *Secretary*

GEOLOGICAL SURVEY

V. E. McKelvey, *Director*

Library of Congress catalog-card No. 73-600206

For sale by the Superintendent of Documents, U.S. Government Printing Office

Washington, D.C. 20402 — Price \$1.05 (paper cover)

Stock Number 2401-02404

CONTENTS

	Page		Page
Abstract	1	Authigenic minerals — Continued	
Introduction	1	Phillipsite	18
Location	1	Potassium feldspar	19
Previous work	2	Quartz	21
Scope of investigation	2	Diagenetic facies	21
Laboratory methods	2	Distribution	21
Acknowledgments	3	Field description	21
Geologic setting	3	Petrography	23
Stratigraphy and lithology of the Big Sandy Formation	4	Nonalcalimic zeolite facies	23
Conglomerate, sandstone, and siltstone	4	Analcime facies	31
Mudstone	6	Potassium feldspar facies	31
Limestone	6	Genesis of authigenic silicate minerals	32
Tuff	8	Interpretation of a saline, alkaline depositional environment for parts of the Big Sandy Formation	33
Authigenic minerals	8	Correlation between the water chemistry of the depositional environment and the authigenic silicate mineralogy	33
Analcime	8	Formation of zeolites from silicic glass	33
Chabazite	10	Reaction of alkalic, silicic zeolites to form analcime	34
Clay minerals	12	Reaction of zeolites to form potassium feldspar	35
Clinoptilolite	13	References cited	35
Erionite	15		
Harmotome	16		
Mordenite	17		
Opal	17		

ILLUSTRATIONS

	Page
FIGURE 1. Index map showing the distribution of the Big Sandy Formation	2
2. Diagrammatic sketch showing X-ray diffractometer patterns of authigenic silicate minerals	3
3. Map of the Big Sandy Formation, showing sample localities	5
4. Generalized columnar section of the Big Sandy Formation	6
5-8. Photomicrographs of analcime, showing:	
5. Thin section of analcimic tuff and individual crystals and clusters of crystals	9
6. Pseudomorphs after prismatic clinoptilolite	10
7. Pseudomorphs of shards	10
8. Irregular patches	11
9. Histogram showing the distribution of Si : Al ratios of analcime in tuff	11
10. Scanning electron micrograph of chabazite-rich tuff, showing rhombohedral morphology of the chabazite	12
11-18. Photomicrographs:	
11. Veinlet of prismatic clinoptilolite	14
12. Cavity lined with phillipsite and clinoptilolite	14
13. Sandstone cemented by finely crystalline clinoptilolite	15
14. Prismatic erionite	16
15. Fibrous erionite	16
16. Radial aggregates of harmotome	17
17. Stubby prismatic crystals of phillipsite	18
18. Spherulitic phillipsite	19
19. Stereographic pair of electron micrographs of potassium feldspar	20
20. Plot of the <i>b</i> and <i>c</i> dimensions of potassium feldspar	22
21. Photomicrograph of spherulitic quartz	23
22. Map showing the diagenetic facies for a composite of all the tuffaceous rocks in the Big Sandy Formation	24
23. Map showing the diagenetic facies for the lower marker tuff of the Big Sandy Formation	25
24-27. Photographs:	
24. Natural exposure of nonalcalimic zeolitic tuff that consists of erionite and clinoptilolite and minor amounts of chabazite	30

	Page
FIGURES 24-27. Photographs — Continued	
25. Natural exposure of chabazite-rich tuff -----	30
26. Natural exposure of erionite-rich upper marker tuff -----	30
27. Natural exposure of analcime-rich lower marker tuff -----	30
28-29. Photomicrographs of nonanalcimic zeolitic tuff, showing preservation of vitroclastic texture -----	31
30. Photomicrograph of nonanalcimic zeolitic tuff, showing pseudomorphs of shards -----	32

TABLES

	Page
TABLE 1. Mineralogic composition of mudstone, as estimated from X-ray diffractometer patterns of bulk samples -----	7
2. Semiquantitative spectrographic analyses of mudstone -----	7
3. Formulas of selected alkalic zeolites -----	8
4. Checklist of associated authigenic silicate minerals in tuffs of the Big Sandy Formation -----	9
5. Chemical analysis and composition of unit cell of analcime -----	11
6. Chemical analysis and composition of unit cell of chabazite -----	12
7. Semiquantitative spectrographic analyses of chabazite-rich and clinoptilolite-rich tuffs -----	13
8. Chemical analysis and composition of unit cell of clinoptilolite -----	15
9. Chemical analysis and composition of unit cell of erionite -----	17
10. Chemical analysis and composition of unit cell of harmotome -----	18
11. Chemical analysis and composition of unit cell of phillipsite -----	19
12. Semiquantitative spectrographic analyses of potassium feldspar-rich tuffs -----	20
13. Unit-cell parameters and boron content of authigenic potassium feldspar -----	21
14. Mineralogic composition of tuffaceous rocks of the Big Sandy Formation, as estimated from X-ray diffractometer patterns of bulk samples -----	26

ZEOLITES AND ASSOCIATED AUTHIGENIC SILICATE MINERALS IN TUFFACEOUS ROCKS OF THE BIG SANDY FORMATION, MOHAVE COUNTY, ARIZONA

By RICHARD A. SHEPPARD and ARTHUR J. GUDE 3D

ABSTRACT

The Big Sandy Formation of Pliocene age covers an area of about 30 square miles in southeastern Mohave County. The formation consists chiefly of nearly flat lying lacustrine rocks that have a maximum exposed thickness of about 245 feet. Lacustrine rocks are mainly mudstone with interbedded tuff and limestone. Mudstone interfingers with coarser clastic rocks in the marginal parts of the formation, and some of these coarser clastic rocks, including sandstone and conglomerate, may be fluvialite. Tuffs make up about 2–3 percent of the exposed stratigraphic section, and they are about 0.5–40 inches thick, although most are less than 6 inches thick. Most tuffs were originally vitric and consisted mainly of silicic, fine to very fine grained ash and a variable percentage of crystal and rock fragments. All the originally vitric material in the tuffaceous rocks is completely altered. This report summarizes the physical properties, chemistry, distribution, and genesis of those silicate minerals that formed in the tuffaceous rocks during diagenesis.

Zeolites, monoclinic potassium feldspar, clay minerals, and silica minerals now compose the altered tuffs. The zeolites are mainly analcime, clinoptilolite, erionite, and chabazite. Phillipsite, mordenite, and harmotome, a rare barium zeolite, are much less abundant. Authigenic clay minerals are nearly ubiquitous and occur in trace to major amounts associated with each of the other silicate minerals. Monomineralic beds of zeolites, especially analcime, and potassium feldspar were recognized, but most zeolitic tuff consists of two or more zeolites. Analcime is associated with each of the other zeolites, and potassium feldspar is associated with analcime and most of the other zeolites. Textural evidence indicates that the zeolites, except analcime, formed directly from the silicic glass by a solution-precipitation mechanism. Neither analcime nor potassium feldspar seems to have formed directly from the silicic glass. Analcime formed from the early zeolite precursors, and potassium feldspar formed from analcime, as well as from the other zeolites.

Three diagenetic facies are recognized in the tuffaceous rocks of the Big Sandy Formation. Those tuffaceous rocks nearest the margin of the formation are characterized by zeolites other than analcime and are termed the "nonanalcimic zeolite facies." Tuffaceous rocks in the central part of the ancient lake basin are characterized by potassium feldspar and are termed the "potassium feldspar facies." Those tuffaceous rocks intermediate in position between the nonanalcimic zeolite facies and the potassium feldspar facies are characterized by analcime and are termed the "analcime facies." The boundaries between the facies are laterally gradational. Although no relict glass was recognized in any of the facies, vitroclastic texture is commonly preserved, especially in tuffs of the nonanalcimic zeolite facies. The distribution and the gradational character of the facies are undoubtedly due to a chemical zonation of the pore water during diagenesis, and this zonation was probably inherited from the chemical zonation that existed in the ancient lake during deposition of the tuffaceous rocks. Those tuffaceous rocks that contain zeolites other than analcime were deposited in the least saline and least alkaline water, near the margin of the lake. Farther basinward, these same rocks are represented by the analcime and potassium feldspar facies because they were deposited in water of in-

creasing salinity and alkalinity. The lake water was probably moderately to highly saline with a pH of 9 or higher, except near the lake margin.

Solution of silicic glass by saline and alkaline pore water during diagenesis provided the materials necessary for the formation of the zeolites and, subsequently, the potassium feldspar. The paragenesis of silicate minerals in the tuffaceous rocks is attributed to chemical variables of the pore water, such as the $\text{Na}^+ + \text{K}^+ : \text{H}^+$ ratio, the Si:Al ratio, the proportion of cations, and the activity of H_2O .

INTRODUCTION

LOCATION

The Big Sandy Formation of Pliocene age is chiefly a lacustrine deposit and is restricted to low elevations in the valley of the Big Sandy River in southeastern Mohave County (fig. 1). Most of the formation is in the east half of T. 16 N., R. 13 W., and the northwestern part of T. 15 N., R. 12 W. The nearest settlement is Wikieup, a small desert town along U.S. Route 93. Kingman is the nearest principal city and is about 40 airline miles to the northwest. The area is shown as a part of the 7½-minute topographic maps of the Greenwood Peak, Gunsight Canyon, Tule Wash, Wikieup, and Wikieup NW quadrangles by the U.S. Geological Survey.

The Big Sandy Formation is in the Basin and Range physiographic province, which is characterized by generally north- to northwest-trending isolated ranges separated by alluvial desert plains. That part of the Basin and Range province in northwestern Arizona has been termed the "Mohave section" by Hayes (1969, p. 35), and the Big Sandy Formation is in the southeastern part of this sub-province. The Big Sandy Formation occupies an intermontane basin which lies between the south end of Hualapai Mountain on the west and Aquarius Cliffs on the east. Most of the peaks surrounding the basin rise to elevations of 5,000–7,000 feet.

The Big Sandy Formation has a northwestward extent along the Big Sandy River of about 12 miles and a width that ranges from about 1.5 to 5.5 miles. The formation underlies an area of about 30 square miles. The lowest exposures, at an elevation of about 1,800 feet, are along the Big Sandy River at the southernmost extent of the formation; the highest exposures, at an elevation of about 2,500 feet, are near the gravel-capped pediments just south of Boner Canyon.

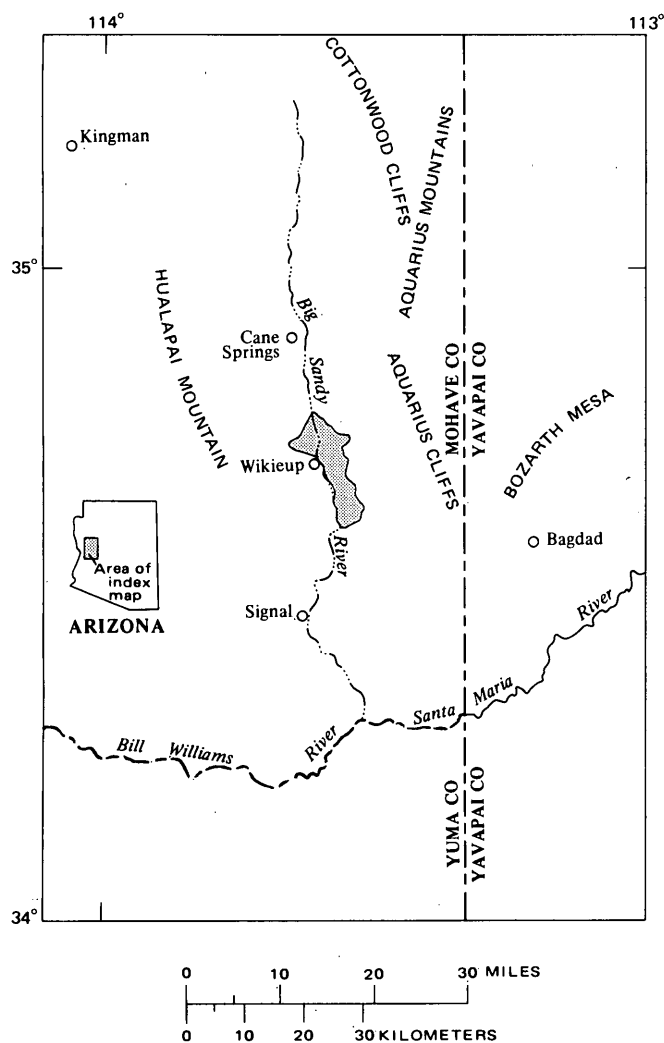


FIGURE 1. — Distribution of the Big Sandy Formation (shaded).

PREVIOUS WORK

Although the lacustrine deposits of late Tertiary age along the Big Sandy River near Wikieup were briefly mentioned as early as 1908 by Lee, the deposits have since received only cursory study. Morrison (1940), as part of a ground-water study of the Big Sandy valley, mapped sedimentary deposits in the valley and included the lacustrine strata in a widespread unit he called "older fill." Ross (1928, 1941) described the zeolite analcime in tuffs of the Big Sandy Formation near Wikieup, and he (1941, p. 627) also described a partial stratigraphic section, about 80 feet thick, of the formation. The formation was formally named and described by Sheppard and Gude (1972a). Short reports on other zeolites in the Big Sandy Formation have been published as part of the present study (Sheppard, 1969; Sheppard and Gude, 1971).

The Big Sandy Formation contains a rich vertebrate fauna, but we are unaware of any published reports on the fossils other than that prepared in conjunction with the pre-

sent study (Sheppard and Gude, 1972a). Several paleontologists from the Frick Laboratory of the American Museum of Natural History have studied the vertebrate fossils from the Big Sandy Formation, but no reports have been published (Ted Galusha, written commun., 1971).

SCOPE OF INVESTIGATION

This investigation of the Big Sandy Formation was made primarily to study the distribution and formation of zeolites and associated authigenic silicate minerals in the tuffaceous beds. Zeolites are common authigenic minerals in tuffaceous rocks of Cenozoic age throughout the desert regions of the Western United States (Sheppard, 1971a). The tuffaceous rocks of the Big Sandy Formation were chosen for detailed study for the following reasons: (1) The formation was subjected to very shallow burial and shows only slight deformation; (2) exposures of the formation are good, and tuffs can be traced throughout most of the extent of the formation; and (3) reconnaissance in 1966 showed an abundance and variety of authigenic silicate minerals in the tuffs. The common occurrence of authigenic analcime and potassium feldspar in the tuffs provided the opportunity to study the genetic relationships of these minerals to the other alkalic, silicic zeolites. Although authigenic clay minerals are common in the tuffaceous rocks, their mineralogy received only cursory examination in this investigation.

Sampling was confined to surface outcrops and weighted heavily in favor of tuffs, although the other rock types were sampled sufficiently to obtain representative material. Weathered surface outcrops were avoided. No cores were available to this investigation.

LABORATORY METHODS

X-ray diffractometer patterns were made of all bulk samples of tuffs. The samples were first ground to a powder, packed in aluminum sample holders, and then exposed to nickel-filtered copper radiation. Relative abundances of authigenic minerals were estimated from the diffractometer patterns by using peak intensities. Estimates are probably less reliable for mixtures containing opal because this material yields a rather poor X-ray record.

Optical studies, made by using immersion oil mounts and thin sections, supplemented the abundance data obtained by X-ray diffraction and provided information on the age relationships of the authigenic minerals. All measurements of the indices of refraction are considered accurate to ± 0.001 .

Most samples of altered tuff contain more than one authigenic mineral. In order to identify each mineral in the diffractometer patterns of bulk samples, the patterns were compared with a "sieve." The sieve, such as that illustrated in figure 2, was prepared from pure mineral separates at the same scale as the patterns of the bulk samples. One mineral at a time could then be sieved from the bulk patterns until all lines were identified. This procedure served to render the

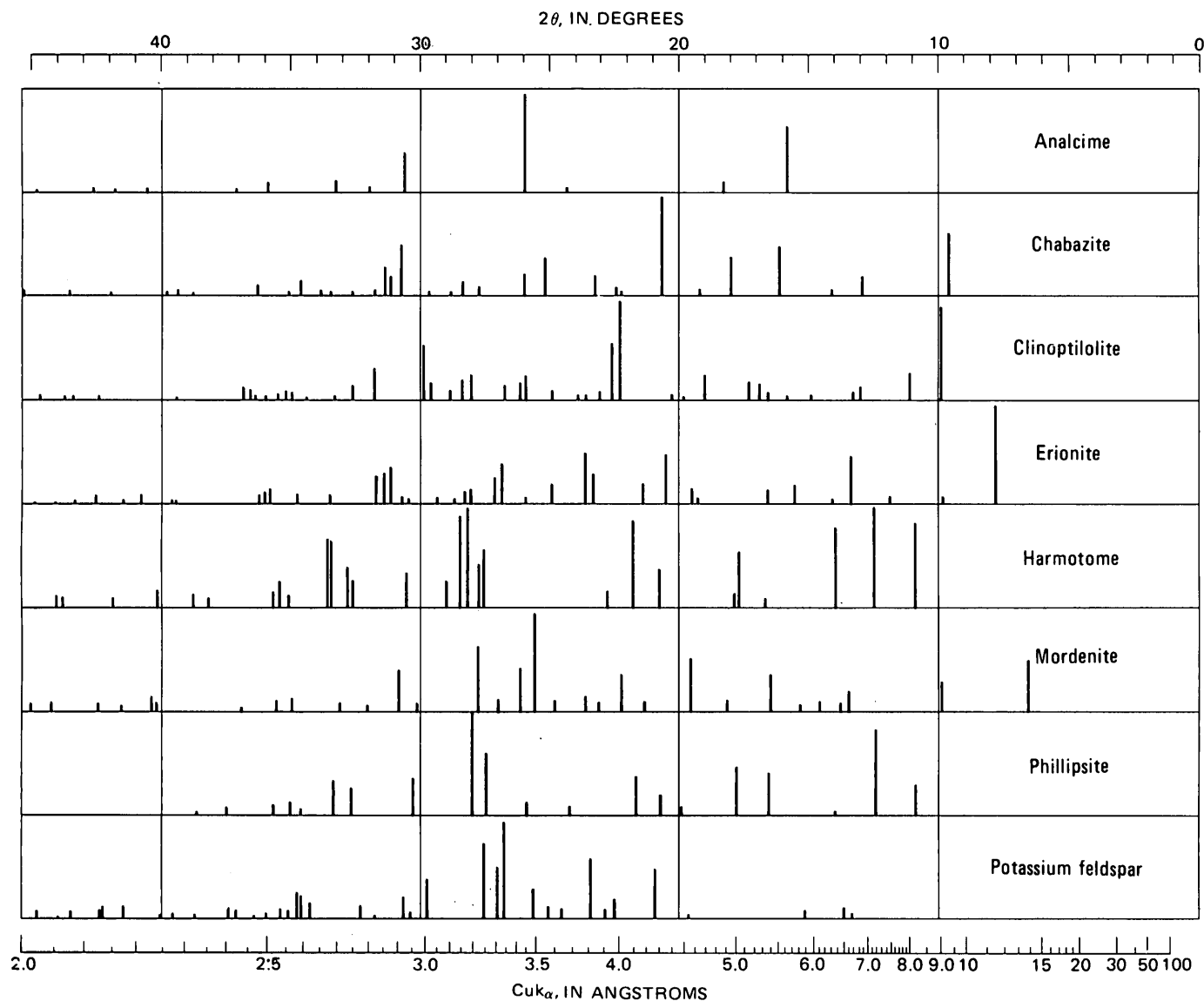


FIGURE 2. — X-ray diffractometer patterns of authigenic silicate minerals. Copper radiation with nickel filter. Relative intensities indicated by height of lines above base line. All samples are from the Big Sandy Formation, except the mordenite, which is from an altered tuff of the Barstow Formation, near Barstow, Calif. (Sheppard and Gude, 1969a).

identifications routine and to help the analyst recognize minor or trace amounts of constituents.

The "pure" mineral separates were prepared for chemical analysis from nearly monomineralic tuffs. The zeolites were separated by crushing the tuff and then disaggregating it in an ultrasonic bath. The zeolites were then concentrated by repeated centrifuging in a heavy-liquid mixture of bromoform and acetone, utilizing the technique described by Schoen and Lee (1964).

ACKNOWLEDGMENTS

Grateful appreciation is expressed to those in the U.S. Geological Survey who provided technical assistance during this study. B. W. Lanthorn, Violet M. Merritt, Wayne Mountjoy, Harriet G. Neiman, George O. Riddle, Van E.

Shaw, and Vertie C. Smith performed the chemical analyses. Mahmood-Uddin Ahmad and Toribio Manzanares, Jr., prepared samples for X-ray diffractometer analysis. Melvin E. Johnson prepared the thin sections. Louise S. Hedricks exercised great patience in the preparation of the photomicrographs.

GEOLOGIC SETTING

The Big Sandy Formation was deposited in a closed basin which formed as a result of the damming of the ancestral Big Sandy River. The mountain ranges surrounding the basin are chiefly Precambrian granitic rocks, although silicic to basaltic volcanic rocks of Tertiary age are common in the mountains along the eastern and southern parts of the basin. The lower slopes of the Aquarius Cliffs are underlain

by tilted Tertiary sedimentary rocks, locally interbedded with basalt flows. The tilted Tertiary sedimentary rocks include both fluvial and lacustrine deposits, some of which have thick interbeds of gypsum at Burro Wash, about 5.5 miles north of Wikieup. A thick conglomerate of Tertiary age overlies the granitic rocks on the eastern flank of Hualapai Mountain. This conglomerate is probably older than the Big Sandy Formation (Sheppard and Gude, 1972a).

Although the ancestral Big Sandy River supplied most of the impounded water in which the Big Sandy Formation was deposited, several major tributaries must have contributed significant quantities of water and detritus. These major tributaries were near the present Natural Corrals Wash on the west and Bull Canyon, Boner Canyon, and Sycamore Creek on the east (fig. 3). As the basin filled with sediment, the lake began to overflow, and the Big Sandy River cut through the barrier. The lake was eventually drained, and the lacustrine sediments were subsequently dissected by the Big Sandy River and its tributaries.

Erosion and dissection of the Big Sandy Formation has proceeded to such a degree that now the area is characterized by badlands and dissected gravel-capped pediments. The Big Sandy River and its mile-wide alluvium-filled channel transects the formation north of Wikieup, but it forms the west boundary of the formation south of Wikieup (fig. 3). Natural exposures of the Big Sandy Formation are mainly in badland areas adjacent to the Big Sandy River or in the steep sides of the numerous washes that head eastward from the river.

Nowhere in the axial part of the basin has the Big Sandy River or its tributaries cut through the basal beds of the Big Sandy Formation. However, small patches of volcanic rocks crop out beneath the formation in marginal parts of the basin near Bitter Creek and midway between Sycamore Creek and Gray Wash (fig. 3). These inliers of older volcanic rocks were probably islands in the lake during much of the deposition of the Big Sandy Formation.

The Big Sandy Formation is only slightly deformed, and it dips generally less than 2°. However, dips up to 10° were measured in Natural Corrals Wash, about 0.5 mile west of U.S. Route 93. Normal faults of slight displacement cut the formation, particularly north of Wikieup. The greatest displacement measured is only 14 feet.

STRATIGRAPHY AND LITHOLOGY OF THE BIG SANDY FORMATION

The Big Sandy Formation, of probable late Pliocene age (Sheppard and Gude, 1972a), consists chiefly of lacustrine rocks that have a maximum exposed thickness of about 245 feet. However, the maximum thickness of the formation is necessarily greater than 245 feet because the basal beds are not exposed. The original thickness must have been even greater because an unknown thickness of the formation was eroded prior to the deposition of the overlying Quaternary

gravel. The formation unconformably overlies Precambrian granitic rocks and unnamed sedimentary and volcanic rocks of Tertiary age.

Green or brown mudstone or a silty, sandy, or calcareous variant is the predominant lithology of the Big Sandy Formation. Limestone and altered tuff beds compose a minor part of the formation, but they are generally very resistant and form conspicuous ledges. The mudstone interfingers marginward with coarser clastic rocks. Some of the coarse clastic beds may be fluvial rather than lacustrine.

A generalized columnar section of the exposed part of the Big Sandy Formation is shown in figure 4. Detailed measured sections of the formation have been published by Sheppard and Gude (1972a). Two of the thickest and most continuous tuffs are in the lower part of the formation and have been given informal field names — lower marker tuff and upper marker tuff. The upper marker tuff is about 35 feet above the lower marker tuff.

CONGLOMERATE, SANDSTONE, AND SILTSTONE

Conglomerate, sandstone, and siltstone occur chiefly in the marginal parts of the formation, especially at its northern extent. These coarse clastic rocks interfinger basinward with mudstone. Thin beds of siltstone and, rarely, sandstone occur locally in the mudstone of the central part of the basin.

Most of the conglomerate is medium to thick bedded and poorly indurated, except where cemented by calcite or zeolites. The pebbles are angular to subrounded, and most are less than 2 inches in diameter. Some beds, however, contain boulders that are as much as 12 inches across. The composition of the pebbles is variable from place to place and reflects the differences in the local source areas. Most beds contain a mixture of volcanic and granitic pebbles, but the volcanic pebbles generally predominate. Some beds contain only volcanic pebbles.

Sandstone and siltstone are brown, green, or gray, and thin to thick bedded, and most are poorly indurated. Cementation is local. The following cements occur, listed in the approximate order of decreasing abundance: Calcite, clay minerals, zeolites (chiefly clinoptilolite or analcime), and opal. Sedimentary structural features other than bedding are rare, but ripple marks and crossbedding are present locally.

The framework constituents of sandstone and siltstone, as well as the sand-size matrix of conglomerate, consist of varying amounts of mineral grains and rock fragments. Sorting is poor, and the clasts have an estimated roundness of 0.2–0.4. The detrital minerals are feldspar and quartz and lesser amounts of biotite, hornblende, epidote, muscovite, magnetite, zircon, apatite, tourmaline, garnet, and sphene, listed in the approximate order of decreasing abundance. Feldspar generally exceeds quartz, and sodic plagioclase exceeds alkali feldspar. Rock fragments are volcanic and lesser amounts of granitic rock, gneiss, schist,

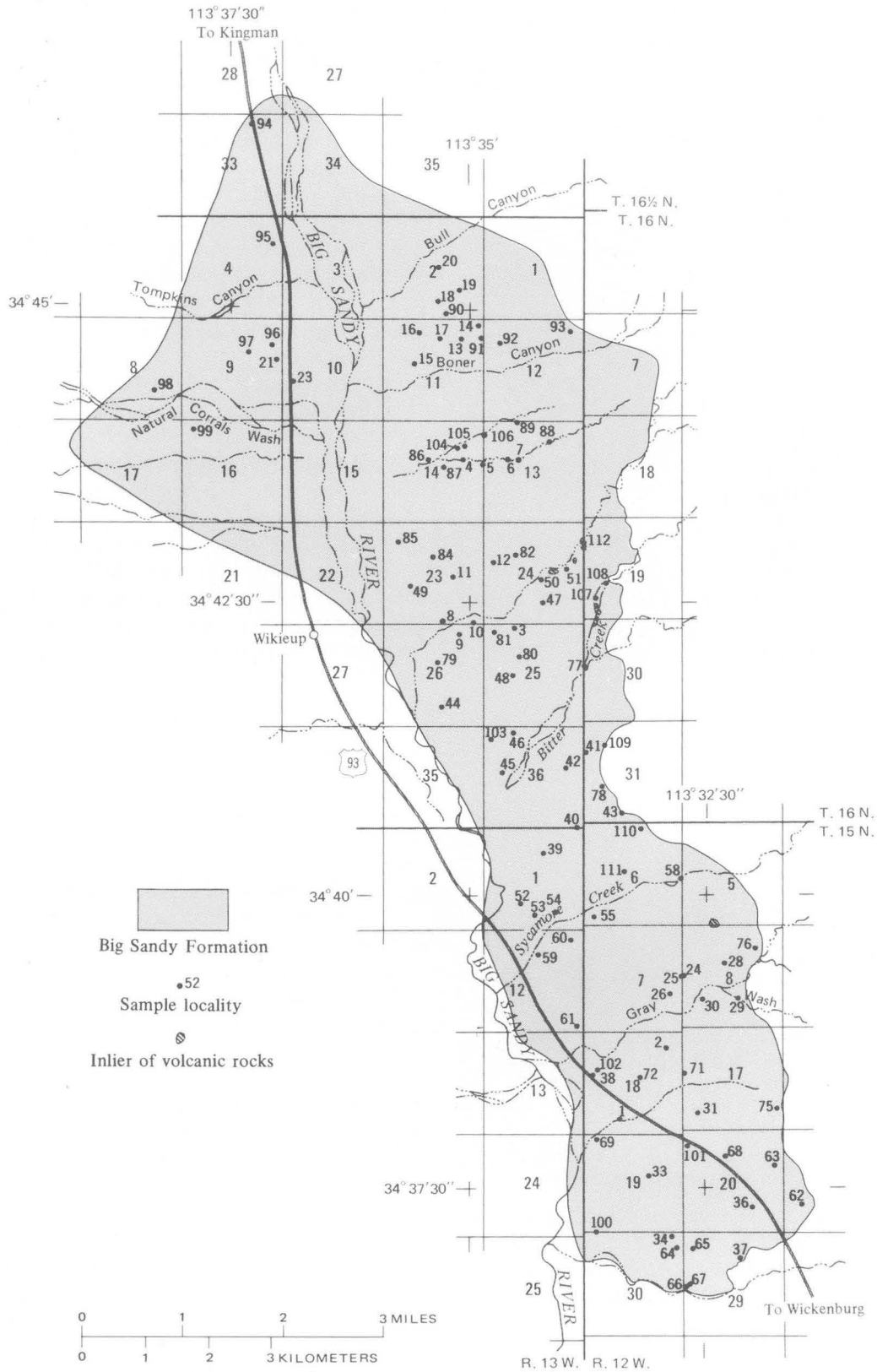


FIGURE 3. — Sample localities in the Big Sandy Formation. X-ray analysis of samples given in table 14.

STRATIGRAPHY AND LITHOLOGY

TABLE 1. — Mineralogic composition of mudstone, as estimated from X-ray diffractometer patterns of bulk samples

[---, looked for but not found; Tr., trace. Clay, 10A includes muscovite, biotite, and illite; clay, 14A includes montmorillonite and mixed-layer montmorillonite-illite]

Field No.	Sample description	X-ray analysis (parts of 10)							
		Clay, 10A	Clay, 14A	Quartz	Plagioclase	Hornblende	Potassium feldspar	Analcime	Calcite
SE¼SW¼ sec. 18, T. 15 N., R. 12 W.									
SW-1-1	Brown mudstone	7	---	---	---	---	2	---	1
SW-1-7	do	1	2	---	Tr.	Tr.	4	1	2
SW-1-11	Greenish-gray mudstone	3	1	---	3	Tr.	3	---	Tr.
SE¼SW¼ sec. 24, T. 16 N., R. 13 W.									
SW-3-1A	Brown mudstone	3	2	3	1	Tr.	---	1	Tr.
SW-3-10A	Gray mudstone	5	---	2	2	---	---	1	---
SW-3-15B	Green mudstone	3	5	---	2	---	---	---	---
NW¼NE¼ sec. 11, T. 16 N., R. 13 W.									
SW-13-1	Brown mudstone	3	3	2	---	Tr.	---	---	2
SW-13-10B	do	2	4	2	2	Tr.	---	---	Tr.

TABLE 2. — Semiquantitative spectrographic analyses of mudstone

[Analyst: Harriet G. Neiman. Localities for samples are given in table 1. Results are to be identified with geometric brackets whose boundaries are 1.2, 0.83, 0.56, 0.38, 0.26, 0.18, 0.12, and so forth, but are reported arbitrarily as midpoints of these brackets, 1, 0.7, 0.5, 0.3, 0.2, 0.15, 0.1, and so forth. The precision of a reported value is approximately plus or minus one bracket at 68-percent confidence, or two brackets at 95-percent confidence. G, greater than 10 percent; N, not detected. The following elements were looked for but not detected: Ag, As, Au, Bi, Cd, Eu, Ge, Hf, In, Mo, P, Pd, Pr, Pt, Re, Sb, Sm, Sn, Ta, Te, Th, Ti, U, W, and Zn]

Field No.	SW-1-1	SW-1-7	SW-1-11	SW-3-1A	SW-3-10A	SW-3-15B	SW-13-1	SW-13-10B
Lab. No.	D142240	D142241	D142242	D142243	D142244	D142246	D142247	D142248
Weight percent								
Si	G	G	G	G	G	G	G	G
Al	10	10	10	7	10	10	7	7
Fe	7	7	7	7	7	7	3	5
Mg	3	2	2	3	3	3	2	3
Ca	3	5	5	5	3	1	G	7
Na	1.5	3	2	3	3	1	3	2
K	7	7	7	5	5	5	5	5
Ti	.5	.5	.5	.7	.5	.5	.5	.5
Parts per million								
B	700	200	500	150	200	300	70	100
Ba	1,000	1,500	700	1,000	1,000	700	500	1,000
Be	2	3	2	2	2	2	1.5	1.5
Ce	200	150	150	150	150	150	200	N
Co	20	15	20	20	15	20	15	20
Cr	150	150	150	200	150	150	50	150
Cu	100	50	50	50	30	100	30	30
Ga	30	20	30	20	30	30	20	30
La	150	100	150	70	100	70	100	100
Li	700	500	500	500	500	700	100	300
Mn	1,500	1,000	1,000	700	1,000	700	1,000	700
Nb	10	10	15	15	15	10	10	10
Nd	150	70	150	70	70	100	100	N
Ni	50	30	30	100	70	70	30	70
Pb	30	20	30	20	15	15	30	15
Sc	20	20	20	20	20	20	20	15
Sr	1,000	1,500	1,000	2,000	2,000	1,000	1,000	1,500
V	300	200	700	200	300	700	100	200
Y	30	30	30	30	20	20	50	30
Yb	3	3	3	3	3	2	3	3
Zr	70	100	100	150	150	70	150	150

deposit. The bedded limestones are light brown or light green, thin to thick bedded, and commonly vuggy and wavy bedded. Beds range in thickness from 0.5 inch to 3 feet, and limestone units are as much as 15 feet thick. Most of the limestone beds contain detrital grains or authigenic silicate minerals. This noncarbonate fraction ranges from less than

1 percent to about 30 percent of the rock. Detrital grains are in all the limestones, but authigenic zeolites and opal are fairly rare. The limestones are finely crystalline, but most have veinlets or cavity fillings of coarsely crystalline calcite that is euhedral to subhedral and white to yellow. No fossils were recognized in any of the limestones.

TUFF

Tuffs in the Big Sandy Formation make up about 2–3 percent of the exposed stratigraphic section (fig. 4). At least 13 tuffs were recognized, and they are about 0.5–40 inches thick, although most are less than 6 inches thick. The thicker tuffs are generally more continuous than the thinner ones. Thin tuffs are commonly single beds, but tuffs more than several inches thick generally consist of multiple beds.

The original textural and structural features of the tuffs are generally preserved even though no vitric material remains. Most tuffs are even bedded; ripple marks or ripple laminations are present but not common. Individual beds of either single bedded or multiple bedded tuffs are commonly graded, being coarser at the base. The lower contact of a tuff is generally sharp, whereas the upper contact is commonly gradational into the overlying rock, regardless of its lithology.

Most of the tuffs originally were vitric and consisted mainly of fine to very fine grained ash and a variable percentage of crystal and rock fragments. The vitric material was of two types — platy bubble-wall shards that formed from the walls and junctions of relatively large broken bubbles, and pumice shards that contained small elongated bubbles. Most tuffs contained both types of shards, but the platy bubble-wall shards were predominant.

Most of the crystal and rock fragments in the tuffs are angular; the fragments range from less than 1 percent to about 50 percent of the rock. Most of the tuffs, however, contain less than 20 percent crystal and rock fragments. Crystal fragments are in excess of rock fragments. Because no fresh glass is attached to the crystal fragments, pyrogenic crystals cannot be positively distinguished from epiclastic ones. However, quartz, sodic plagioclase, biotite, hornblende, sanidine, clinopyroxene, zircon, apatite, and magnetite are presumed to be pyrogenic. Crystal fragments of epiclastic origin are epidote, muscovite, microcline, garnet, chlorite, and sphene, which were probably derived from the granitic terranes surrounding the basin. Many of the presumably pyrogenic crystals listed above could also have been derived from the older volcanic and granitic rocks that are marginal to the Big Sandy Formation.

The rock fragments are volcanic and granitic rocks and a minor amount of gneiss. Volcanic rock fragments are spherulitic and hyalopilitic lavas. The rock fragments could have been torn from the vent area during eruption of the ash, or they could be epiclastic.

Some tuffs and the lower part of some tuffs are the result of ash falls directly into a lake. Other tuffs (particularly the upper part of most tuffs) consist of reworked ash mixed with epiclastic grains derived from the highlands surrounding the basin. Most of these tuffs, or parts of tuffs, contain an abundance of granitic rock fragments and crystal fragments of epidote and microcline.

The original composition of the ash is unknown, but the

presumed pyrogenic crystal fragments in the tuffs indicate a silicic composition, probably rhyolitic or dacitic.

The two marker tuffs (fig. 4) are the thickest and most continuous tuffs in the Big Sandy Formation. The lower marker tuff crops out from the NE¼ sec. 30, T. 15 N., R. 12 W., northward to the NE¼ sec. 14, T. 16 N., R. 13 W., and can be recognized wherever its stratigraphic interval is exposed. The thickness of the lower marker tuff is 6–39 inches but commonly is 18–24 inches. The tuff is at least 30 inches thick in sec. 18 and the N½ sec. 19, T. 15 N., R. 12 W. The upper marker tuff occurs about 35 feet stratigraphically above the lower marker tuff and crops out from the NW¼ sec. 29, T. 15 N., R. 12 W., northward to the NW¼ sec. 25, T. 16 N., R. 13 W. Although the stratigraphic interval of the upper marker tuff is exposed farther north, the upper marker tuff was not recognized north of sec. 25, T. 16 N., R. 13 W. The thickness of the upper marker tuff is 9–40 inches, and it seems to gradually decrease from south to north.

AUTHIGENIC MINERALS

ANALCIME

Analcime, commonly referred to as analcite, is one of the more abundant zeolites in sedimentary rocks. Analcime has an ideal formula of $\text{NaAlSi}_2\text{O}_6 \cdot \text{H}_2\text{O}$, but the analcime of sedimentary rocks is generally more siliceous (table 3). Since its discovery in the Green River Formation (Bradley, 1928) and in the tuffs of the Big Sandy Formation (Ross, 1928), analcime has been reported in sedimentary rocks that are diverse in age, lithology, and depositional environment (Hay, 1966). Analcime occurs in rocks that range in age from Pennsylvanian to Holocene, but it is especially common relative to the other zeolites in rocks of Mesozoic age, particularly those older than Cretaceous. Saline lacustrine deposits, regardless of age, very commonly contain analcime. Analcime, unlike the other zeolites in sedimentary rocks, does occur in rocks that lack evidence of vitric material, and is apparently a common constituent of saline, alkaline soils, such as those in southern California (Baldar and Whittig, 1968).

TABLE 3. — *Formulas of selected alkalic zeolites*

[Formulas are standardized in terms of a sodium end member that has one aluminum atom]

Name	Dominant cations	Formula
Analcime	Na	$\text{NaAlSi}_{1.5-2.9}\text{O}_{5.0-7.8} \cdot 0.8-1.3\text{H}_2\text{O}$
Chabazite	Na, Ca, K	$\text{NaAlSi}_{1.5-4.1}\text{O}_{5.0-10.2} \cdot 2.7-4.7\text{H}_2\text{O}$
Clinoptilolite	Na, K, Ca	$\text{NaAlSi}_{3.4-5.5}\text{O}_{8.8-13.0} \cdot 2.5-4.0\text{H}_2\text{O}$
Erionite	Na, K, Ca	$\text{NaAlSi}_{2.9-3.8}\text{O}_{7.8-9.6} \cdot 2.4-3.4\text{H}_2\text{O}$
Harmotome	Ba, Na, K	$\text{NaAlSi}_{2.0-2.8}\text{O}_{6.0-7.6} \cdot 2.5-3.0\text{H}_2\text{O}$
Mordenite	Na, Ca, K	$\text{NaAlSi}_{4.5-5.1}\text{O}_{11.0-12.6} \cdot 3.2-3.5\text{H}_2\text{O}$
Phillipsite	Na, K, Ca	$\text{NaAlSi}_{1.3-3.4}\text{O}_{4.6-8.8} \cdot 1.7-3.3\text{H}_2\text{O}$

Analcime is a very common zeolite in the tuffs of the Big Sandy Formation, where it ranges from trace amounts to nearly 100 percent of the rock. The analcime is associated with each of the other zeolites, but its association with mordenite and chabazite is rare (table 4). Analcime is also commonly associated with authigenic potassium feldspar,

TABLE 4. — Checklist of associated authigenic silicate minerals in tuffs of the Big Sandy Formation

[X, mineral pair associated; O, mineral pair not associated. Data compiled from X-ray diffractometer patterns of bulk samples. Clay minerals include 10A and 14A types; quartz includes epiclastic, pyrogenic, and authigenic crystals]

	Analcime	Chabazite	Clay minerals	Clinoptilolite	Erionite	Harmotome	Mordenite	Opal	Phillipsite	Potassium feldspar	Quartz
Analcime	—	X	X	X	X	X	X	X	X	X	X
Chabazite	X	—	X	X	X	X	O	O	X	X	X
Clay minerals	X	X	—	X	X	X	X	X	X	X	X
Clinoptilolite	X	X	X	—	X	X	X	X	X	X	X
Erionite	X	X	X	X	—	X	X	X	X	X	X
Harmotome	X	X	X	X	X	—	O	O	O	O	X
Mordenite	X	O	X	X	X	O	—	O	O	O	X
Opal	X	X	X	X	X	O	O	—	O	X	X
Phillipsite	X	X	X	X	X	O	O	O	—	X	X
Potassium feldspar	X	X	X	X	X	O	O	X	X	—	X
Quartz	X	X	X	X	X	X	X	X	X	X	—

quartz, and clay minerals. The association of analcime with potassium feldspar is particularly common.

Analcime has three modes of occurrence in the tuffs of the Big Sandy Formation — (1) subhedral to euhedral crystals, (2) pseudomorphs of shards and early authigenic

silicate minerals, and (3) irregular patches. Subhedral to euhedral crystals are by far the most common occurrence of analcime. The subhedral to euhedral crystals (fig. 5) range in size from 5µm to 50µm, although most are 20µm to 40µm. The analcime is pale tan in transmitted light and generally milky in reflected light, owing to abundant minute inclusions. Analcime pseudomorphs after prismatic clinoptilolite (fig. 6) and analcime pseudomorphs of shards (fig. 7) are sparse in the altered tuffs. Petrographic evidence indicates that the shards were first pseudomorphed by an earlier zeolite, generally clinoptilolite, and then were replaced by analcime. The irregular patches of analcime are colorless and are as much as about 1 mm (fig. 8). This analcime replaced earlier authigenic silicate minerals, completely obliterating the vitroclastic texture.

The index of refraction of analcime from the Big Sandy Formation ranges from 1.483 to 1.488. Saha (1959) showed that the index of refraction of synthetic analcimes decreases with increasing Si:Al ratio. The above indices are consistent with fairly high Si:Al ratios.

A new chemical analysis of analcime from the Big Sandy Formation is given in table 5. The analcime was separated

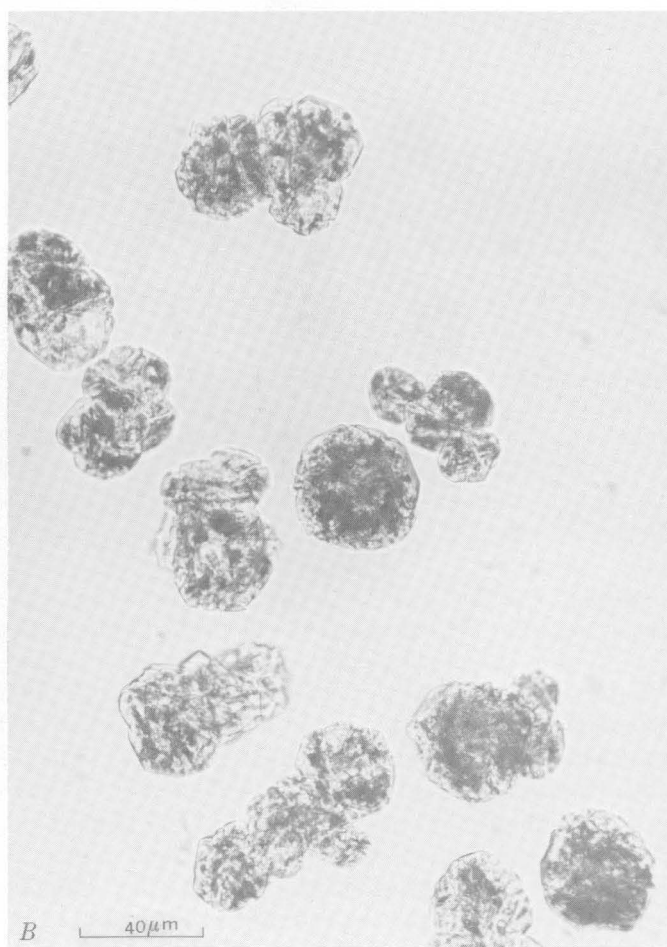
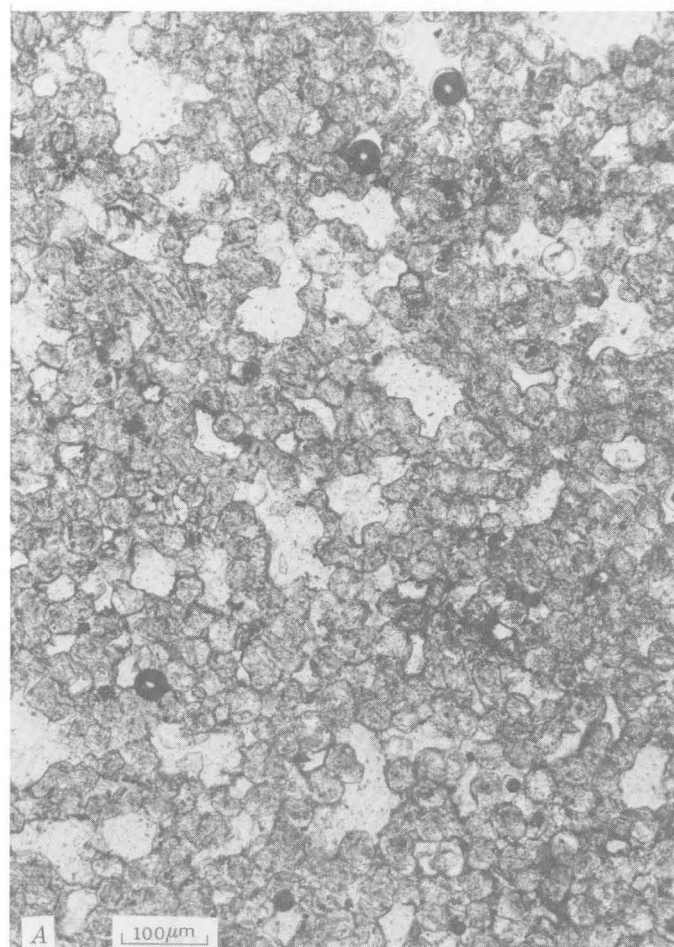


FIGURE 5. — Subhedral to euhedral analcime. A, Thin section of analcime tuff. Irregular light areas are pores in the tuff. Unpolarized light. B, Individual crystals and clusters of crystals separated from an analcime tuff. Unpolarized light.



FIGURE 6. — Analcime pseudomorphs after prismatic clinoptilolite. Light areas are quartz. Unpolarized light.

from a nearly monomineralic portion of the lower marker tuff. The analyzed analcime contained less than 2 percent minute clay mineral inclusions, but the analysis was not corrected for them. The composition of the unit cell based on 96 oxygen atoms is also given in table 5 and shows a Si:Al+Fe⁺³ ratio of 2.49. Sodium is greatly in excess of the other cations.

Ross (1928) has published two analyses of analcime separated from a tuff collected near Wikieup. The exact locality and stratigraphic position of the tuff are unknown, but the tuff probably was the lower marker tuff. Both separates contained minor impurities of clay minerals and opal. The uncorrected analyses showed Si:Al+Fe⁺³ ratios of about 2.6 and 2.8.

The composition of analcime from 55 other samples was determined indirectly by measurement of the displacement of the (639) peak, utilizing the data of Saha (1959, 1961) for synthetic analcimes and the determinative curve of Shepard and Gude (1969a). Saha showed that the (639) peak falls at higher angles (degrees 2θ, CuKα₁ radiation) for analcimes of higher silicon content. Displacement of the (639) peak of analcime was measured against the (331) peak

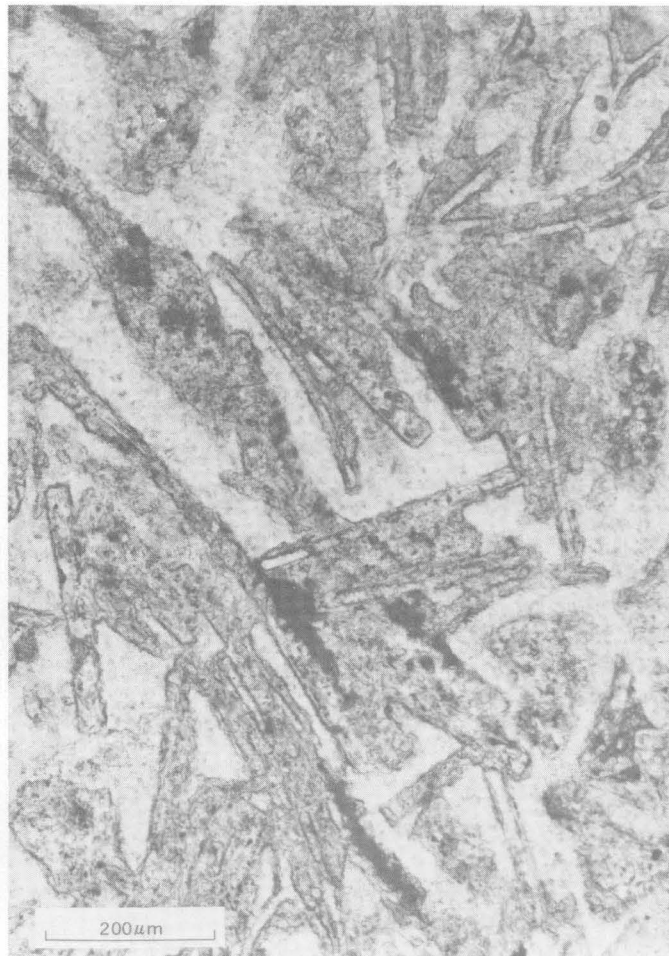


FIGURE 7. — Analcime pseudomorphs of shards (dark). Light areas are quartz. Unpolarized light.

of a silicon internal standard. The analcimes from tuffs of the Big Sandy Formation show a compositional range from about (NaAl)_{14.2}Si_{33.8}O₉₆·nH₂O to (NaAl)_{12.7}Si_{35.3}O₉₆·nH₂O. The Si:Al ratio of the analcimes ranges from about 2.4 to 2.8; the distribution for the 55 samples is shown in figure 9. Nearly half the samples have a Si:Al ratio of 2.5–2.6. Coombs and Whetten (1967) studied analcimes from many sedimentary environments and determined a range in Si:Al of about 2.0–2.7. Analcimes in tuffs of the Eocene Green River Formation of Wyoming have Si:Al ratios of about 2.0–2.9 (Iijima and Hay, 1968), and analcimes in tuffs of the Miocene Barstow Formation of California have Si:Al ratios of about 2.2–2.8 (Shepard and Gude, 1969a).

CHABAZITE

Chabazite was unknown in sedimentary deposits before 1964, when it was discovered by Hay (1964, p. 1377) in tuffs and tuffaceous clays at Olduvai Gorge, Tanzania. Since then, authigenic chabazite has been recognized in tuffs from California, Nevada, Oregon, Wyoming, and several localities in Arizona. Most of the occurrences are in lacustrine rocks of late Cenozoic age. Chabazite has an ideal formula of Ca₂Al₄Si₈O₂₄·12H₂O, but natural

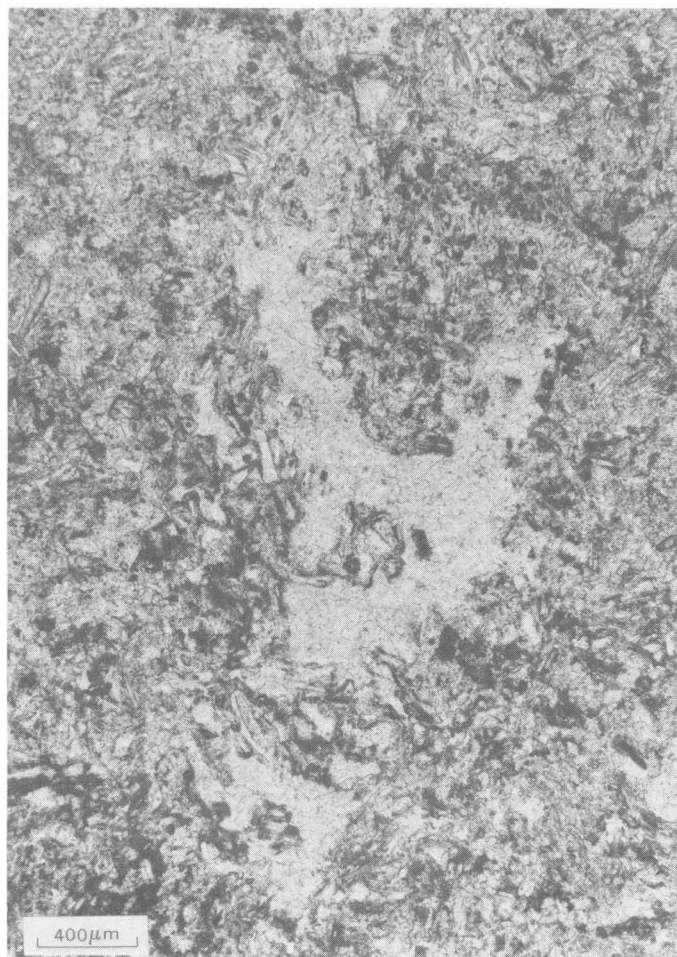


FIGURE 8. — Irregular patches of analcime (light), which have replaced erionite and chabazite pseudomorphs of shards. The vitroclastic texture is preserved where analcime is absent. Unpolarized light.

chabazites show considerable variation in cation content and in Si:Al ratio (table 3).

The chabazite in the Big Sandy Formation occurs in nearly monomineralic beds, but generally it is associated with clay minerals, other zeolites, or potassium feldspar of authigenic origin (table 4). Chabazite has not been recognized in association with opal or mordenite, and its association with potassium feldspar or analcime is rare. Erionite and clinoptilolite are the zeolites that are most commonly associated with chabazite. The chabazite occurs as aggregates of equidimensional crystals that are anhedral to euhedral. Some of the chabazite crystals have a rhombohedral morphology (fig. 10), as shown by electron microscopy. The crystals range in maximum dimension from less than 2 μ m to 40 μ m, but most are less than 20 μ m.

The mean index of refraction of chabazite from the Big Sandy Formation ranges from 1.468 to 1.474, and the birefringence is about 0.002. This compares with a range of 1.470–1.494 given by Deer, Howie, and Zussman (1963, p. 387) for chabazite from nonsedimentary environments. The indices for the Big Sandy chabazites are, however, similar to

TABLE 5. — Chemical analysis and composition of unit cell of analcime

[Analyst: Vertie C. Smith, except for Na₂O, K₂O, and SrO determined by atomic absorption by Violet Merritt and for BaO determined gravimetrically by V. E. Shaw. The Al₂O₃ content includes P₂O₅, and the Fe₂O₃ content represents total iron. Field No. SW-3-2A. Lab. No. D138981. Loc. 3 (fig. 3), NE¼NW¼ sec. 25, T. 16 N., R. 13 W.]

Chemical analysis	
Constituent	Weight percent
SiO ₂	58.62
Al ₂ O ₃	19.37
Fe ₂ O ₃	.95
MgO	.23
CaO	.15
BaO	.02
SrO	.02
Na ₂ O	11.00
K ₂ O	.38
H ₂ O ⁺	7.91
H ₂ O ⁻	.31
TiO ₂	.06
Total	99.02

Composition of unit cell	
[Ti was omitted in calculation of the unit cell]	
Constituent	Atoms per unit cell
Si	34.32
Al	13.37
Fe ⁺³	.42
Mg	.20
Ca	.09
Ba	.00
Sr	.01
Na	12.49
K	.28
H ₂ O ⁺	15.45
H ₂ O ⁻	.60
O	96.00
Si+Al+Fe ⁺³	48.11
Si:Al+Fe ⁺³	2.49

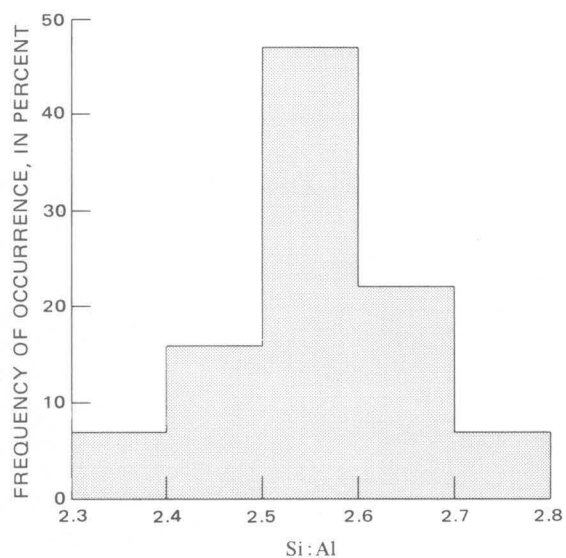


FIGURE 9. — Distribution of Si:Al ratios of analcime in 55 samples of tuff from the Big Sandy Formation. The Si:Al ratios were determined from X-ray diffractometer data by measurement of the displacement of the (639) peak of analcime.

those for siliceous chabazites from silicic tuffs (Sheppard and Gude, 1970).

A chemical analysis of chabazite from the Big Sandy Formation is given in table 6. The chabazite was separated from



FIGURE 10. — Scanning electron micrograph of chabazite-rich tuff, showing rhombohedral morphology of the chabazite. Prismatic crystals (bottom) are erionite. Electron micrograph by Frederick A. Mumpton.

a nearly monomineralic part of a thin tuff stratigraphically higher than the upper marker tuff. The analysis was calculated into atoms per unit cell, on the basis of 72 oxygen atoms, and is also given in table 6. Divalent cations exceed monovalent ones, and the Si:Al+Fe⁺³ ratio is 3.27.

Ideal chabazite has a Si:Al+Fe⁺³ ratio of 2, and most of the chabazites from mafic igneous rocks have a ratio near 2. The few analyzed chabazites from sedimentary rocks, however, have Si:Al+Fe⁺³ ratios greater than 3. A calcic chabazite from a silicic tuff in the John Day Formation of Oregon was recently analyzed and has a Si:Al+Fe⁺³ ratio of about 4.1 (Sheppard and Gude, 1970), higher than that for any previously analyzed chabazite.

Chabazite from the Big Sandy Formation has higher potassium and magnesium contents than previously analyzed chabazites from sedimentary rocks. Semiquantitative spectrographic analyses (table 7) of five chabazite-rich tuffs from the Big Sandy Formation suggest that the relatively high potassium and magnesium contents are characteristic for these chabazites. The spectrographic analyses were performed on bulk samples that contained at least 90 percent chabazite. The spectrographic analyses also confirm that the divalent cations are in excess of the monovalent ones, although the sodium contents are higher than the sodium

TABLE 6. — Chemical analysis and composition of unit cell of chabazite

[Analyst: George Riddle, except for BaO and SrO determined by atomic absorption by Wayne Mountjoy, Field No. W7-6A, Lab. No. D102734, Loc. 6 (fig. 3), SE¼NW¼ sec. 13, T. 16 N., R. 13 W.]

Chemical analysis	
Constituent	Weight percent
SiO ₂	56.39
Al ₂ O ₃	13.36
Fe ₂ O ₃	2.01
FeO	.02
MgO	2.79
CaO	2.46
BaO	.03
SrO	.13
Na ₂ O	.72
K ₂ O	2.50
H ₂ O+	12.80
H ₂ O-	5.78
TiO ₂	.38
P ₂ O ₅	.05
MnO	.06
Total	99.48
Composition of unit cell	
[Fe ⁺² , Ti, P, and Mn were omitted in calculation of the unit cell]	
Constituent	Atoms per unit cell
Si	27.46
Al	7.67
Fe ⁺³	.74
Mg	2.02
Ca	1.28
Ba	.01
Sr	.04
Na	.68
K	1.55
H ₂ O+	20.79
H ₂ O-	9.39
O	72.00
Si+Al+Fe ⁺³	35.87
Si:Al+Fe ⁺³	3.27

content given in table 6. The barium content of sample No. W8-95B seems anomalously high for a chabazite from any geologic setting (Passaglia, 1970).

Cell parameters for the analyzed Big Sandy chabazite were obtained by a least-squares refinement of X-ray powder diffractometer data, utilizing the U.S. Geological Survey's FORTRAN IV Computer Program W9214. The hexagonal cell parameters are $a=13.735\pm 0.004$ Å, $c=14.840\pm 0.006$ Å, and $V=2,424.3\pm 1.2$ Å³. These cell dimensions are smaller than those of chabazites from mafic igneous rocks. Most chabazites from mafic igneous rocks have a cell volume of 2,470–2,490 Å³, but siliceous chabazites from silicic tuffaceous sedimentary rocks have a cell volume of 2,410–2,430 Å³ (Sheppard and Gude, 1970). Thus, the relatively small cell of the Big Sandy chabazite is consistent with a siliceous composition.

CLAY MINERALS

Most tuffs in the Big Sandy Formation contain authigenic clay minerals, but no attempt was made to study the clay mineralogy in detail. The clay minerals are associated with all the other authigenic silicate minerals, and their content is generally less than 40 percent of the tuff. Examination of X-ray diffractometer patterns of bulk samples indicated that 10A and 14A clay minerals occur in the tuffs. The 14A clay minerals are probably mont-

TABLE 7. — *Semiquantitative spectrographic analyses of chabazite-rich and clinoptilolite-rich tuffs*

[Analyst: Harriet G. Neiman. Results are to be identified with geometric brackets whose boundaries are 1.2, 0.83, 0.56, 0.38, 0.26, 0.18, 0.12, and so forth, but are reported arbitrarily as midpoints of these brackets, 1, 0.7, 0.5, 0.3, 0.2, 0.15, 0.1, and so forth. The precision of a reported value is approximately plus or minus one bracket at 68-percent confidence, or two brackets at 95-percent confidence. G, greater than 10 percent; N, not detected but below limit of determination. The following elements were looked for but not detected: Ag, As, Au, Bi, Cd, Eu, Ge, Hf, In, Mo, P, Pd, Pr, Pt, Re, Sb, Sm, Sn, Ta, Te, Th, Tl, U, W, and Zn]

	Chabazite-rich tuff				Clinoptilolite-rich tuff						
	1	2	3	4	5	6	7	8	9	10	11
Weight percent											
Si -----	G	G	G	G	G	G	G	G	G	G	G
Al -----	7	5	7	7	7	7	7	7	10	10	7
Fe -----	3	2	2	2	2	1	3	2	2	2	1
Mg -----	1.5	1.5	1.5	2	1	.5	1.5	1	1.5	1	.3
Ca -----	5	3	3	3	3	1.5	2	5	3	3	1.5
Na -----	2	2	1	2	3	.7	2	3	2	3	3
K -----	2	3	1	2	2	5	3	3	3	3	2
Ti -----	.3	.15	.2	.15	.2	.1	.3	.2	.1	.2	.1
Parts per million											
B -----	N	20	N	L	N	100	50	50	30	20	70
Ba -----	300	1,500	150	300	15,000	1,500	1,000	3,000	1,500	1,500	15,000
Be -----	1	3	N	N	1	2	1.5	1	1	1	2
Ce -----	L	150	N	N	N	200	N	N	N	N	L
Co -----	5	5	7	5	5	N	7	5	L	3	N
Cr -----	50	50	15	20	7	7	100	50	15	10	1.5
Cu -----	20	10	10	15	15	5	20	70	10	10	1
Ga -----	20	10	10	15	10	15	15	15	15	20	15
La -----	50	50	N	30	50	150	50	30	30	N	70
Li -----	70	N	N	70	N	200	100	300	300	500	100
Mn -----	300	300	150	200	300	100	500	300	150	200	100
Nb -----	L	10	L	N	N	10	10	N	N	L	15
Nd -----	70	N	N	N	N	70	N	N	N	N	N
Ni -----	5	10	10	15	5	N	10	7	7	5	N
Pb -----	15	15	L	10	10	10	15	30	10	10	15
Sc -----	15	7	10	10	10	5	15	10	7	15	N
Sr -----	2,000	3,000	1,000	1,000	7,000	30,000	1,500	15,000	5,000	1,500	15,000
V -----	100	100	70	200	15	100	150	1,000	70	300	30
Y -----	30	15	10	10	20	20	15	20	10	20	20
Yb -----	5	1	1.5	1.5	3	2	1.5	3	L	3	1.5
Zr -----	150	150	200	150	150	150	100	100	100	200	150

Analysis Field No.	Lab. No.	Locality	Analysis Field No.	Lab. No.	Locality
1. W7-14B	D142252	NE¼NE¼ sec. 11, T. 16 N., R. 13 W.	7. SW-67-2	D142250	NW¼SW¼ sec. 29, T. 15 N., R. 12 W.
2. W7-19B	D142253	NW¼SE¼ sec. 2, T. 16 N., R. 13 W.	8. SW-67-9A	D142251	NW¼SW¼ sec. 29, T. 15 N., R. 12 W.
3. W8-89A	D142260	SE¼SW¼ sec. 12, T. 16 N., R. 13 W.	9. W7-28A	D142256	SE¼NW¼ sec. 8, T. 15 N., R. 12 W.
4. W8-89C	D142261	SE¼SW¼ sec. 12, T. 16 N., R. 13 W.	10. W7-36B	D142257	SW¼SE¼ sec. 20, T. 15 N., R. 12 W.
5. W8-95B	D142262	NE¼NE¼ sec. 4, T. 16 N., R. 13 W.	11. W7-42B	D142258	SE¼NE¼ sec. 36, T. 16 N., R. 13 W.
6. SW-26-9B	D142249	NE¼SE¼ sec. 7, T. 15 N., R. 12 W.			

morillonite and mixed-layered montmorillonite-illite. Examination of thin sections of tuffs proved that much of the 10A clay mineral shown in the X-ray diffractometer patterns is biotite of detrital or pyrogenic origin. Some of the 10A clay mineral, however, is authigenic illite, inasmuch as the (001) peak is broad, and biotite is absent in the thin sections. Montmorillonite seems to be the most abundant authigenic clay mineral in the tuffs.

CLINOPTILOLITE

Clinoptilolite is a member of the heulandite structural group. Although there is still disagreement on the distinction between these closely related zeolites, most workers have considered clinoptilolite to be the silica-rich (Hey and Bannister, 1934; Mumpton, 1960) and alkali-rich (Mason and Sand, 1960) member (table 3). Indices of refraction and response to thermal treatment have also been used to dis-

tinguish clinoptilolite from heulandite. However, some members of the heulandite structural group from sedimentary rocks display anomalous optical properties and thermal behavior and cannot be classified conveniently as clinoptilolite or heulandite (Shepard, 1961; Hay, 1963). Furthermore, siliceous, but calcic, clinoptilolite has recently been discovered in volcanic rocks of Bulgaria (Kirov, 1965) and Italy (Alietti, 1967).

The original description of clinoptilolite is of material from amygdaloids in a basaltic rock from Wyoming (Pirsson, 1890; Schaller, 1932). Subsequent occurrences of clinoptilolite have been reported chiefly from sedimentary rocks, especially those originally rich in silicic vitric material. Clinoptilolite is the zeolite most often reported from sedimentary rocks in recent years, and it occurs in many rock types from lacustrine, fluvial, and marine environments. Although clinoptilolite is most abundant in



FIGURE 11. — Veinlet of prismatic clinoptilolite (light) in zeolitic tuff consisting chiefly of finely crystalline phillipsite (dark). Unpolarized light.

rocks of Cenozoic age, it has been reported in New Mexico in rocks as old as Jurassic (Sheppard, 1971b).

Clinoptilolite is a very common zeolite in the tuffs of the Big Sandy Formation, and it is associated with all the other authigenic silicate minerals. The clinoptilolite content ranges from trace amounts to nearly 100 percent of the tuffs. Clinoptilolite occurs as prismatic (fig. 11) or platy (fig. 12) crystals that are $2\mu\text{m}$ to $375\mu\text{m}$ long; most, however, are $10\mu\text{m}$ to $30\mu\text{m}$ long. The clinoptilolite occurs as pseudomorphs after shards and as fillings of veinlets or irregular cavities in the tuffs. Small prismatic clinoptilolite also serves as a cement in some sandstones (fig. 13).

Most of the clinoptilolite has a mean index of refraction of 1.475–1.483 and a birefringence of about 0.003. The clinoptilolite has parallel extinction and is length slow. Some large clinoptilolite crystals, particularly those larger than about $80\mu\text{m}$, are length fast or zoned, having a length-slow core and a length-fast rim. The rim of zoned crystals commonly has an index of refraction that is as much as 0.006 higher than that of the core. Rarely, large crystals of clinoptilolite show oscillatory zoning.

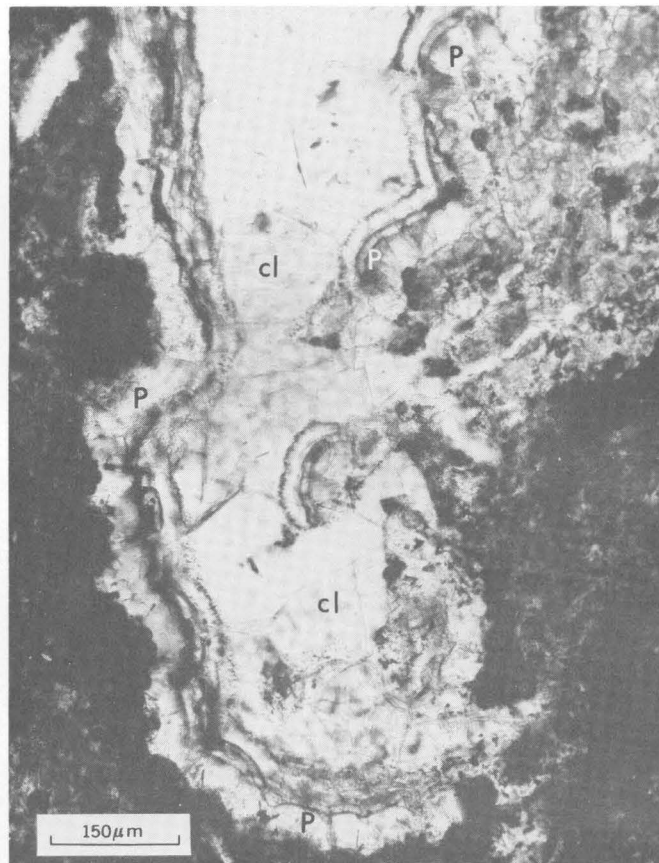


FIGURE 12. — Irregular cavity that was first lined with fibrous to spherulitic phillipsite (P) and then filled by platy clinoptilolite (cl). Unpolarized light.

An analysis of clinoptilolite from the Big Sandy Formation is given in table 8. The clinoptilolite was separated from a nearly monomineralic part of a thin tuff that is stratigraphically higher than the upper marker tuff. The analysis was calculated in atoms per unit cell, on the basis of 72 oxygen atoms, and is also given in table 8. Divalent cations exceed monovalent ones, and the $\text{Si}:\text{Al}+\text{Fe}^{+3}$ ratio is 4.03. Most clinoptilolites from sedimentary rocks are alkalic and have $\text{Si}:\text{Al}+\text{Fe}^{+3}$ ratios of 4–5 (Sheppard, 1971b). Thus, this specimen from the Big Sandy Formation is unusual because of its high calcium and magnesium contents.

Semiquantitative spectrographic analyses of six bulk samples of clinoptilolite-rich tuffs are given in table 7. All the tuffs contain at least 90 percent clinoptilolite. The spectrographic analyses suggest that the chemical analysis given in table 8 is not characteristic of the clinoptilolites in the Big Sandy Formation. Most of the spectrographic analyses show clinoptilolite to be rich in alkalis, rather than in alkaline earths. The spectrographic analyses also show that the clinoptilolite-rich tuffs contain as much as 1.5 weight percent barium and as much as 3.0 weight percent strontium.

The strontium content of clinoptilolites separated from



FIGURE 13. — Sandstone cemented by finely crystalline clinoptilolite (cl). Unpolarized light.

the strontium-rich tuffs was determined by semiquantitative spectrographic analysis and showed a range of 0.7–3.0 weight percent. The mean index of refraction of these strontium-rich clinoptilolites is 1.488–1.496, which is significantly higher than that for clinoptilolites containing less than 0.5 weight percent strontium.

ERIONITE

Erionite was considered to be an extremely rare mineral before the work of Deffeyes (1959a, b) and Regnier (1960), who showed it to be a common authigenic zeolite in the altered silicic tuffs of lacustrine deposits in north-central Nevada. Since then, erionite has been recognized in silicic bedded tuffs from many of our Western States (Sheppard 1971a). Erionite, like chabazite, has not been reported from sedimentary rocks older than Eocene. Most occurrences of erionite are in upper Cenozoic lacustrine deposits.

Erionite in the tuffs of the Big Sandy Formation occurs as nearly monomineralic beds or in association with the other zeolites, clay minerals, opal quartz, or potassium feldspar of authigenic origin (table 4). The association of erionite with clinoptilolite is especially common, but the associations

TABLE 8. — Chemical analysis and composition of unit cell of clinoptilolite

[Analyst: George Riddle, except for BaO and SrO determined by atomic absorption by Wayne Mountjoy. Field No. W7-6B. Lab. No. D102735. Loc. 6 (fig. 3), SE¼NW¼ sec. 13, T. 16 N., R. 13 W.]

Chemical analysis	
Constituent	Weight percent
SiO ₂	62.78
Al ₂ O ₃	12.33
Fe ₂ O ₃	1.41
FeO	.00
MgO	1.99
CaO	3.10
BaO	.13
SrO	.40
Na ₂ O	.63
K ₂ O	1.67
H ₂ O ⁺	9.08
H ₂ O ⁻	5.36
TiO ₂	.28
P ₂ O ₅	.03
MnO	.09
Total	99.28
Composition of unit cell	
[Ti, P, and Mn were omitted in calculation of the unit cell]	
Constituent	Atoms per unit cell
Si	28.76
Al	6.65
Fe ⁺³	.48
Mg	1.36
Ca	1.52
Ba	.02
Sr	.11
Na	.56
K	.97
H ₂ O ⁺	13.87
H ₂ O ⁻	8.19
O	72.00
Si+Al+Fe ⁺³	35.89
Si:Al+Fe ⁺³	4.03

with mordenite, opal, and potassium feldspar are rare. Unlike the woolly-appearing erionite from the type locality near Durkee, Oreg. (Eakle, 1898), most of the Big Sandy erionite is prismatic (fig. 14) or acicular (fig. 15). The erionite commonly forms a network of unoriented prismatic crystals or aggregates of radiating acicular crystals. Spherulites of erionite are relatively rare in the tuffs of the Big Sandy Formation. Individual crystals range in length from 10µm to 130µm, but most are 20µm to 60µm long.

Indices of refraction of the Big Sandy erionite are: ω=1.464–1.467 and ε=1.467–1.470; birefringence is 0.003. Erionite has parallel extinction and is length slow. The indices are in the upper part of the range, 1.458–1.470, given by Sheppard and Gude (1969b) for other erionites from silicic tuffs.

A chemical analysis of erionite that was separated from a nearly monomineralic part of the upper marker tuff is given in table 9. The analysis was corrected for minor calcite impurities associated with the erionite. The corrected analysis was then calculated into atoms per unit cell, on the basis of 72 oxygen atoms, and is also given in table 9. Monovalent cations exceed divalent ones, and the Si:Al+Fe⁺³ ratio is 3.77. The molecular ratio Al₂O₃+Fe₂O₃: (Ca, Mg, Ba, Sr, Na₂, K₂) O for zeolites should be unity; however, this ratio

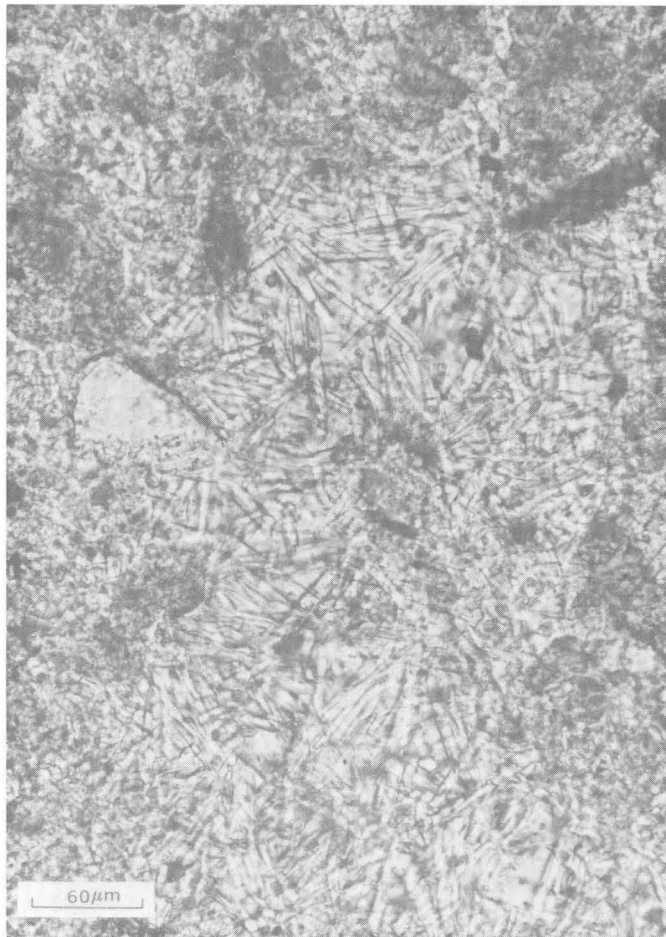


FIGURE 14. — Network of prismatic erionite. Unpolarized light.

for the Big Sandy erionite is about 0.6. Thus, the cation oxides are greatly in excess of $\text{Al}_2\text{O}_3 + \text{Fe}_2\text{O}_3$, and the analysis is unfortunately of poor quality. Compared with analyses of other erionites from silicic tuffs (Sheppard and Gude, 1969b), the Big Sandy erionite has high contents of magnesium and strontium.

Cell parameters for the analyzed Big Sandy erionite were obtained by a least-squares refinement of X-ray powder diffractometer data, utilizing the U.S. Geological Survey's FORTRAN IV Computer Program W9214. The hexagonal cell parameters are $a = 13.219 \pm 0.002$ Å, $c = 15.040 \pm 0.005$ Å, and $V = 2.276.0 \pm 1.0$ Å³. Inasmuch as the cell volume of erionite seems to decrease with increasing Si:Al+Fe⁺³ ratio (Sheppard and Gude, 1969b), this cell volume for the Big Sandy specimen is compatible with a relatively high Si:Al+Fe⁺³ ratio.

HARMOTOME

Harmotome, probably the most common of the barium-rich zeolites, has been reported from a variety of metamorphic and igneous rocks throughout the world (Deer and others, 1963, p. 399). It is also commonly associated with metallic ore deposits. Although harmotome is a relatively rare zeolite in sedimentary rocks, it has been

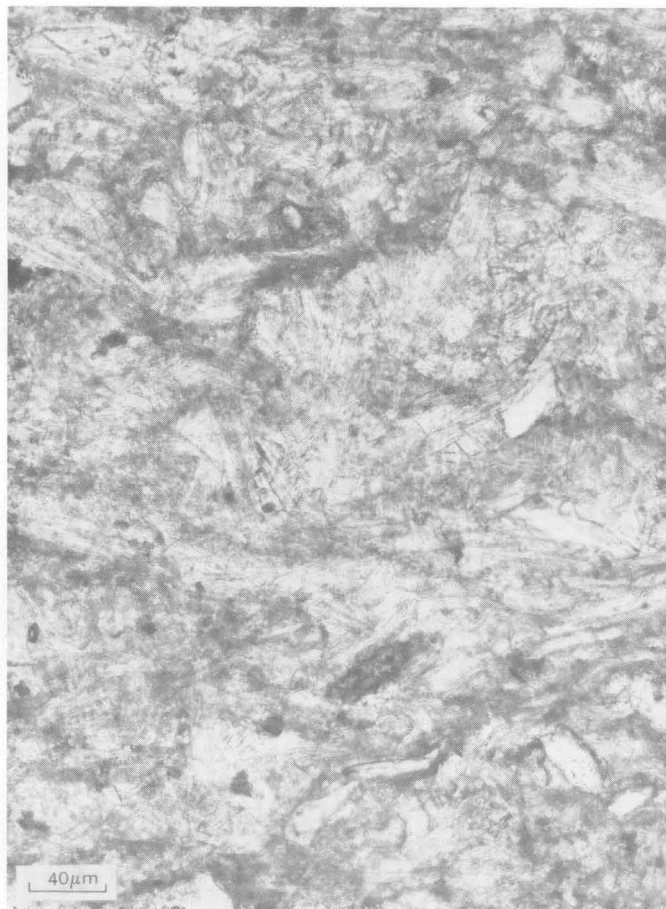


FIGURE 15. — Fibrous erionite in zeolitic tuff. Vitroclastic texture is vaguely preserved. Unpolarized light.

reported from deep-sea sediments (Morgenstein, 1967) and from lacustrine rocks in the Green River Formation and the Big Sandy Formation (Sheppard and Gude, 1971).

Harmotome occurs in tuffs of the Big Sandy Formation in amounts ranging from a trace to about 40 percent of the rock. It is associated with authigenic clay minerals and one or more of the following zeolites: analcime, chabazite, clinoptilolite, and erionite. X-ray diffractometer patterns of harmotome-bearing tuffs also show quartz, but examination of thin sections indicated that the quartz is pyrogenic or detrital rather than authigenic.

The harmotome in tuffs of the Big Sandy Formation occurs as prismatic or acicular crystals that are about 2 μm to 30 μm long. The crystals are commonly in radial aggregates (fig. 16) or small spherulites that are 20 μm to 30 μm in diameter. The harmotome has a mean index of refraction of 1.506 and is length fast.

A chemical analysis of harmotome from the Big Sandy Formation was corrected for analcime impurities (Sheppard and Gude, 1971) and is given in table 10. The harmotome was separated from a thin tuff stratigraphically higher than the upper marker tuff. The corrected analysis was calculated into atoms per unit cell, on the basis of 32 oxygen

TABLE 9. — Chemical analysis and composition of unit cell of erionite

[a column, uncorrected analysis; b column, analysis corrected for CO₂ plus equivalent CaO to make calcite. Analyst: George Riddle, except for BaO and SrO determined by atomic absorption by Wayne Mountjoy. Field No. SW-26-4C. Lab. No. D102733. Loc. 26 (fig. 3), NE¼SE¼ sec. 7, T. 15 N., R. 12 W.]

Chemical analysis		
Constituent	a (weight percent)	b (weight percent)
SiO ₂	58.37	59.93
Al ₂ O ₃	12.23	12.55
Fe ₂ O ₃	1.44	1.48
FeO	.09	.09
MgO	3.98	4.08
CaO	1.72	.77
BaO	.13	.13
SrO	1.14	1.17
Na ₂ O	1.72	1.76
K ₂ O	6.12	6.28
H ₂ O+	6.22	6.39
H ₂ O-	4.96	5.10
TiO ₂	.14	.14
P ₂ O ₅	.11	.11
MnO	.02	.02
CO ₂	.76	---
Total	99.15	100.00

Composition of unit cell

[Fe²⁺, Ti, P, and Mn were omitted in calculation of the unit cell]

Constituent	Atoms per unit cell
Si	27.47
Al	6.78
Fe ⁺³	.51
Mg	2.79
Ca	.38
Ba	.02
Sr	.31
Na	1.56
K	3.67
H ₂ O+	9.77
H ₂ O-	7.80
O	72.00
Si+Al+Fe ⁺³	34.76
Si:Al+Fe ⁺³	3.77

atoms, and is also given in table 10. Monovalent cations are in excess of divalent ones, and the Si:Al+Fe⁺³ ratio is 2.47. The ideal formula for harmotome is Ba₂Al₄Si₁₂O₃₂·12H₂O, but most of the natural specimens contain substantial amounts of alkalis, mainly sodium. This harmotome from the Big Sandy Formation is the most sodium-rich and barium-poor harmotome thus far reported from any geologic environment. The deviation in composition of the Big Sandy harmotome from the ideal formula can be approximated by about 0.54 Na₂(K₂) replacement of 0.54 Ba(Sr,Ca,Mg), and by about 0.69 Na(K)Al(Fe⁺³) replacement of 0.69 silicon.

Cell parameters for the Big Sandy harmotome were obtained by a least-squares refinement of X-ray powder diffractometer data, utilizing the U.S. Geological Survey's FORTRAN IV Computer Program W9214. The resulting monoclinic cell parameters for the analyzed specimen are a=9.921±0.004 Å, b=14.135±0.009 Å, c=8.685±0.006 Å, β=124°55'±2', and V=998.59±0.76 Å³.

MORDENITE

Mordenite has been confused with clinoptilolite or heulandite in sedimentary rocks because of similar indices of refraction and chemistry. X-ray diffractometer techniques, however, are adequate for positive identification (fig.

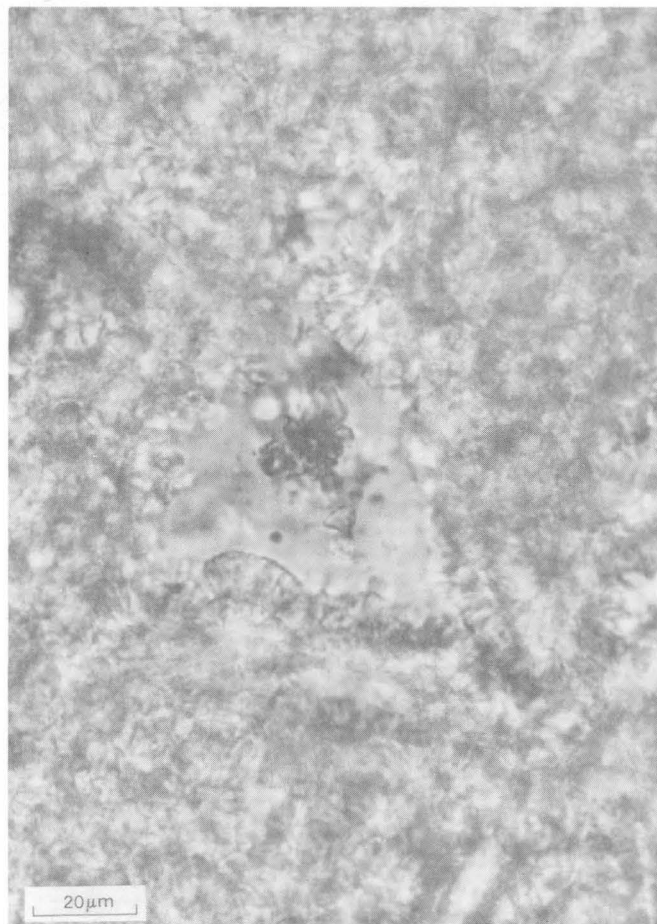


FIGURE 16. — Radial aggregates of harmotome, Unpolarized light.

2). In recent years, mordenite has commonly been identified in Cenozoic tuffaceous rocks of the Western United States (Sheppard, 1971a).

Mordenite is the least common zeolite in tuffs of the Big Sandy Formation, and it has been recognized only from X-ray diffractometer patterns of bulk samples. The mordenite ranges in abundance from trace amounts to about 30 percent of the tuff and is associated with authigenic clay minerals, analcime, clinoptilolite, erionite, and quartz. Mordenite is most commonly associated with clinoptilolite and quartz.

Inasmuch as mordenite occurs in small amounts and is invariably associated with some other authigenic zeolite in the tuffs, no attempt was made to separate material for chemical analysis. Mordenites generally have a range in Si:Al+Fe⁺³ ratio of about 4.5–5.3 and generally have alkalis in excess of alkaline earths.

OPAL

Opal is difficult to recognize in the tuffs because of its isotropic and nondescript character. The opal is colorless to pale brown in thin section and has an index of refraction of 1.43–1.46. Most of the opal is milky in reflected light. Most identifications of opal in tuffs of the Big Sandy Formation

TABLE 10. — *Chemical analysis and composition of unit cell of harmotome*

[Analyst: Vertie C. Smith, except for SrO determined by atomic absorption by Violet Merritt. The Al₂O₃ content includes P₂O₅ and the Fe₂O₃ content represents total iron. Analysis was corrected for analcime impurities and recalculated to 100 percent (Sheppard and Gude, 1971). Field No. W7-44. Lab. No. D13893. Loc. 44 (fig. 3), SW¹/₄SE¹/₄ sec. 26, T. 16 N., R. 13 W.]

Chemical analysis	
Constituent	Weight percent
SiO ₂	49.97
Al ₂ O ₃	15.15
Fe ₂ O ₃	3.15
MgO	1.52
CaO	.64
BaO	8.75
SrO	.10
Na ₂ O	3.33
K ₂ O	2.24
H ₂ O ⁺	8.72
H ₂ O ⁻	6.16
TiO ₂	.27
Total	100.00

Composition of unit cell	
[Ti was omitted in calculation of the unit cell]	
Constituent	Atoms per unit cell
Si	11.31
Al	4.04
Fe ⁺³	.54
Mg	.51
Ca	.16
Ba	.78
Sr	.01
Na	1.46
K	.65
H ₂ O ⁺	6.58
H ₂ O ⁻	4.65
O	32.00
Si+Al+Fe ⁺³	15.89
Si:Al+Fe ⁺³	2.47

are based on X-ray diffractometer data of bulk samples. The opal has characteristically broad peaks at the following *d* spacings: 4.28 Å, 4.08 Å, and 2.50 Å. Opal is associated with authigenic clay minerals, potassium feldspar, quartz, and each of the zeolites except harmotome, mordenite, and phillipsite. Associations of opal with analcime, clinoptilolite, and potassium feldspar are especially common. The abundance of opal ranges from trace amounts to about 70 percent of the tuffs; however, most tuffs contain no more than 20 percent opal.

PHILLIPSITE

Phillipsite has long been known to occur in deposits on the sea floor (Murray and Renard, 1891, p. 400–411). Since the discovery by Deffeyes (1959a) of phillipsite in lacustrine tuffs of Nevada, this zeolite has been commonly reported as a rock-forming constituent in tuffaceous rocks of the Western United States. Phillipsite occurs in sedimentary rocks that range in age from Cretaceous to Holocene, but it is especially common in lacustrine deposits of late Cenozoic age, particularly those deposits of saline, alkaline lakes.

Phillipsite in the Big Sandy Formation occurs in nearly monomineralic beds, but most of it is associated with authigenic clay minerals, potassium feldspar, quartz, or

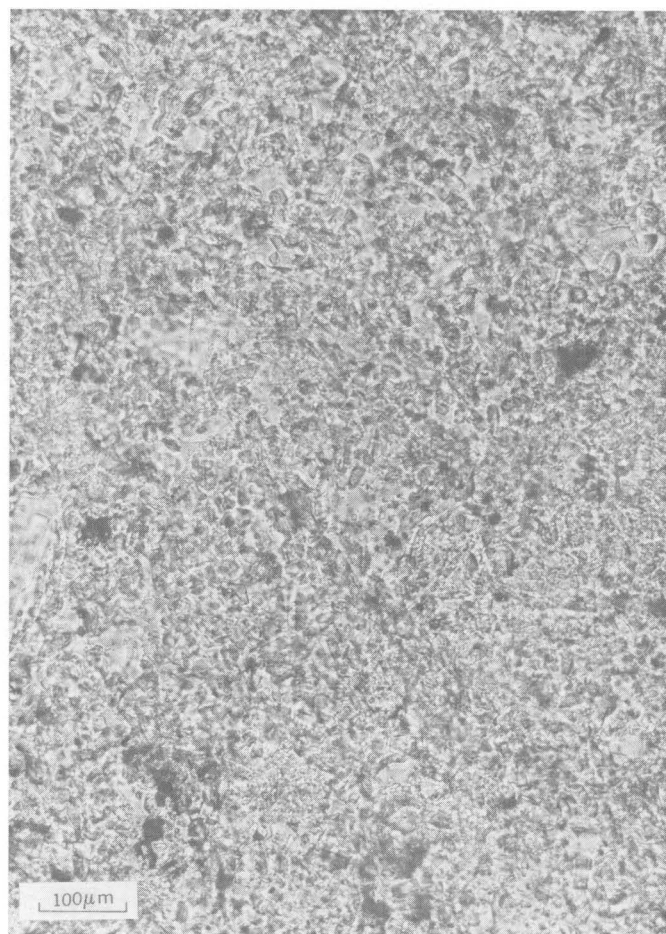


FIGURE 17. — Stubby prismatic crystals of phillipsite. Unpolarized light.

other zeolites (table 4). Phillipsite has not been recognized in association with harmotome, mordenite, or opal and its association with potassium feldspar is rare. Clinoptilolite is the zeolite that is most commonly associated with phillipsite in tuffs of the Big Sandy Formation. The phillipsite occurs as stubby prismatic crystals or as spherulites. The prismatic crystals (fig. 17) range in length from less than 2 μm to 25 μm, but most are less than 15 μm long. The spherulites (fig. 18), some of which are hollow, are 25 μm to 100 μm in diameter. Some spherulites show concentric zoning.

The mean index of refraction of the Big Sandy phillipsite is 1.459–1.468, and the birefringence is about 0.002. The phillipsite has parallel extinction and is length slow. Indices of refraction for phillipsites from various rock types range from about 1.44 to 1.51 and seem to vary inversely with the Si:Al+Fe⁺³ ratio (Hay, 1964). The indices of the Big Sandy phillipsites are consistent with those of siliceous phillipsites from saline lacustrine deposits.

A chemical analysis of phillipsite from the Big Sandy Formation is given in table 11. The phillipsite was separated from a nearly monomineralic thin tuff that is stratigraphically higher than the upper marker tuff. The analysis was calculated into atoms per unit cell, on the basis

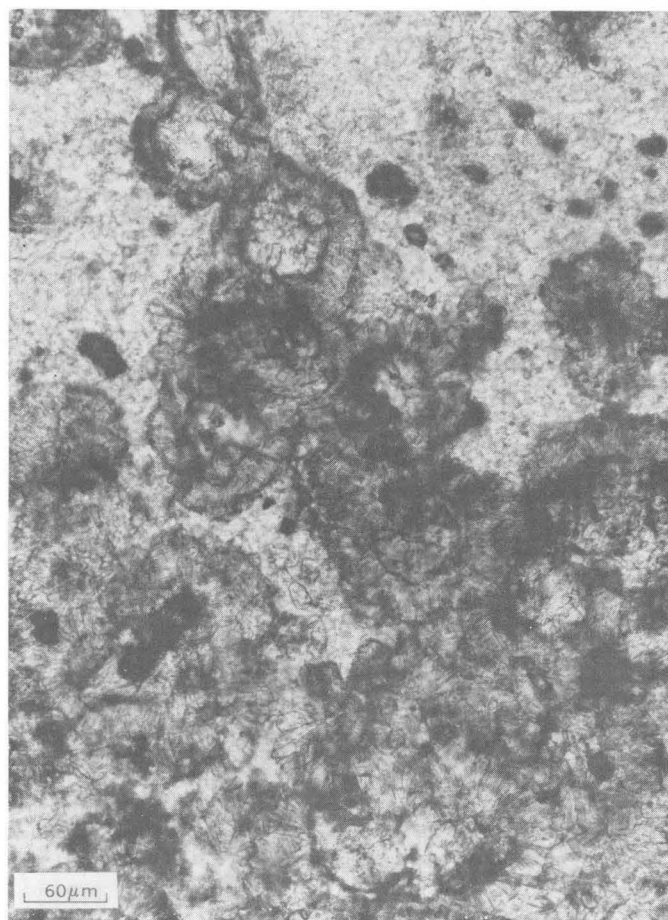


FIGURE 18. — Spherulitic phillipsite. Unpolarized light.

of 32 oxygen atoms, and is also given in table 11. Monovalent cations greatly exceed divalent ones, and the Si:Al+Fe⁺³ ratio is 3.37. The high Si:Al+Fe⁺³ ratio, the high contents of alkalis, and the excess of sodium over potassium are characteristic of authigenic phillipsites formed in silicic tuffs of saline lacustrine deposits (Sheppard and others, 1970).

POTASSIUM FELDSPAR

Potassium feldspar occurs as an authigenic mineral in sedimentary rocks that are diverse in lithology, depositional environment, and age (Hay, 1966). The authigenic potassium feldspar is a pure or nearly pure potassium variety and occurs as authigenic crystals, overgrowths on detrital or pyrogenic feldspars, and replacements of detrital and pyrogenic plagioclase. In the tuffs of the Big Sandy Formation, the potassium feldspar occurs chiefly as authigenic crystals and only rarely replaces plagioclase. The authigenic potassium feldspar occurs in nearly monomineralic beds or is associated with authigenic clay minerals, opal, quartz, and each of the zeolites except harmotome and mordenite (table 4). The association of authigenic potassium feldspar with analcime is especially common.

Potassium feldspar occurs in the tuffs as low birefringent

TABLE 11. — Chemical analysis and composition of unit cell of phillipsite

[Analyst: George Riddle, except for BaO and SrO determined by atomic absorption by Wayne Mountjoy. Field No. W7-25A. Lab. No. D102736. Loc. 25 (fig. 3). SE¼NE¼ sec. 7, T. 15 N., R. 12 W.]

Chemical analysis	
Constituent	Weight percent
SiO ₂	56.55
Al ₂ O ₃	13.23
Fe ₂ O ₃	1.67
FeO	.07
MgO	2.47
CaO	.48
BaO	.35
SrO	.39
Na ₂ O	4.14
K ₂ O	5.69
H ₂ O+	6.83
H ₂ O-	6.74
TiO ₂	.20
P ₂ O ₅	.19
MnO	.02
Total	99.02

Composition of unit cell [Fe ⁺² , Ti, P, and Mn were omitted in calculation of the unit cell]	
Constituent	Atoms per unit cell
Si	12.02
Al	3.31
Fe ⁺³	.26
Mg	.78
Ca	.11
Ba	.03
Sr	.05
Na	1.70
K	1.54
H ₂ O+	4.84
H ₂ O-	4.78
O	32.00
Si+Al+Fe ⁺³	15.59
Si:Al+Fe ⁺³	3.37

aggregates of crystals. These crystals range in maximum dimension from about 2µm to 14µm; however, most are 4µm to 8µm long. Paul D. Blackmon, using electron microscopy, has shown that the crystals are subhedral to euhedral (fig. 19). The feldspar is identical in habit and size with authigenic potassium feldspar from altered silicic tuffs of Pleistocene Lake Tecopa, Calif. (Sheppard and Gude, 1968), and altered tuffs of the Miocene Barstow Formation (Sheppard and Gude, 1969a). The mean index of refraction is about 1.522 and indicates a pure or nearly pure potassium feldspar. Other optical parameters could not be determined because of the small size of the feldspar crystals.

Semiquantitative spectrographic analyses of six bulk samples of potassium feldspar-rich tuff are given in table 12. All the samples contain more than 90-percent feldspar, as determined by X-ray diffraction. The analyses confirm that the feldspar is highly potassic and also show that the samples are relatively rich in boron. Quantitative spectrographic analyses for boron for the six bulk samples are given in table 13. The boron content ranges from 660 to 2,300 ppm, but it is generally greater than 1,500 ppm. The absence of a boron-rich mineral from these nearly monomineralic tuffs suggests that the boron is in the authigenic potassium feldspar.

Cell parameters for the six specimens of authigenic

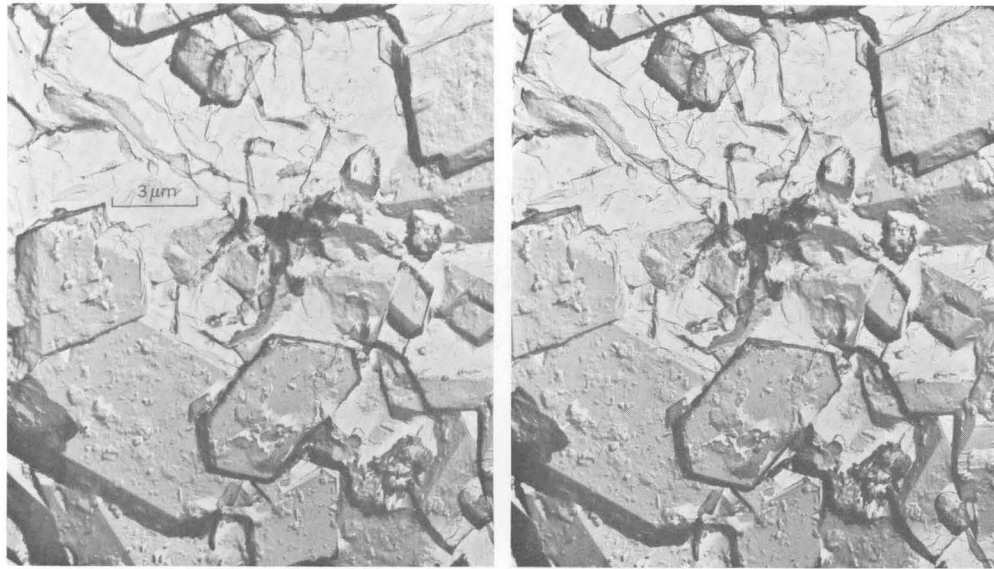


FIGURE 19. — Stereographic pair of electron micrographs, showing subhedral to euhedral authigenic potassium feldspar in the lower marker tuff. Electron micrographs by Paul D. Blackmon.

TABLE 12. — *Semiquantitative spectrographic analyses of potassium feldspar-rich tuffs*

[Analyst: B. W. Lanthorn. Results are to be identified with geometric brackets whose boundaries are 1.2, 0.83, 0.56, 0.38, 0.26, 0.18, 0.12, and so forth, but are reported arbitrarily as mid-points of these brackets, 1, 0.7, 0.5, 0.3, 0.2, 0.15, 0.1, and so forth. The precision of a reported value is approximately plus or minus one bracket at 68-percent confidence, or two brackets at 95-percent confidence. G, greater than 10 percent; N, not detected; L, detected but below limit of determination. The following elements were looked for but not detected: Ag, As, Au, Bi, Cd, Eu, Ge, Hf, In, P, Pd, Pr, Pt, Re, Sb, Sm, Sn, Ta, Te, Th, Tl, U, W, and Zn]

	1	2	3	4	5	6
Weight percent						
Si -----	G	G	G	G	G	G
Al -----	10	7	10	10	G	7
Fe -----	3	2	3	2	2	1
Mg -----	.3	.3	.7	.7	.3	.15
Ca -----	.3	.15	.3	1.5	.7	.2
Na -----	.2	.7	.5	.3	.7	.5
K -----	7	7	10	10	10	7
Ti -----	.07	.03	.2	.05	.05	.03
Parts per million						
B -----	1,000	1,000	300	1,500	700	1,000
Ba -----	150	70	150	150	700	150
Be -----	7	5	2	3	5	3
Ce -----	150	150	N	200	L	L
Co -----	7	N	7	N	5	N
Cr -----	15	5	15	7	10	20
Cu -----	30	10	7	10	50	20
Ga -----	30	20	30	30	30	20
La -----	150	100	70	150	50	100
Li -----	500	200	200	500	200	200
Mn -----	500	300	300	300	500	150
Mo -----	7	7	10	5	7	5
Nb -----	30	20	L	20	15	20
Nd -----	70	70	N	100	70	70
Ni -----	10	N	7	5	7	L
Pb -----	15	10	20	15	15	L
Sc -----	7	5	10	5	5	N
Sr -----	500	200	150	300	500	150
V -----	500	200	70	150	150	30
Y -----	20	50	10	30	15	L
Yb -----	1.5	7	1.5	3	1.5	1
Zr -----	150	200	150	150	100	150

NUMBERS AND LOCALITIES OF SAMPLES

1. Field No. SW-2-1B. Lab. No. D141570. Locality: NE $\frac{1}{4}$ NE $\frac{1}{4}$ sec. 18, T. 15 N., R. 12 W.
2. Field No. W7-40A. Lab. No. D141571. Locality: SE $\frac{1}{4}$ SE $\frac{1}{4}$ sec. 36, T. 16 N., R. 13 W.
3. Field No. W7-41A. Lab. No. D141572. Locality: SW $\frac{1}{4}$ NW $\frac{1}{4}$ sec. 31, T. 16 N., R. 12 W.
4. Field No. W7-45B. Lab. No. D141574. Locality: SW $\frac{1}{4}$ NW $\frac{1}{4}$ sec. 36, T. 16 N., R. 13 W.
5. Field No. W8-54D. Lab. No. D141575. Locality: SW $\frac{1}{4}$ SE $\frac{1}{4}$ sec. 1, T. 15 N., R. 13 W.
6. Field No. W8-72D. Lab. No. D141577. Locality: SW $\frac{1}{4}$ NE $\frac{1}{4}$ sec. 18, T. 15 N., R. 12 W.

potassium feldspar from tuffs of the Big Sandy Formation are given in table 13. The monoclinic cell parameters were obtained by a least-squares refinement of X-ray powder diffractometer data, utilizing the U.S. Geological Survey's FORTRAN IV Computer Program W9214. The cell parameters show the following range: $a=8.570-8.591$ A, $b=12.960-12.990$ A, $c=7.163-7.173$ A, $\beta=115^{\circ}54.7'-116^{\circ}4.6'$, and $V=715.61-718.99$ A³.

The b and c cell dimensions for the six Big Sandy authigenic potassium feldspars are plotted in figure 20, the potassic portion of Wright and Stewart's (1968) $b-c$ quadrilateral for alkali feldspars. All the authigenic feldspars plot near the high sanidine corner but well within the quadrilateral. This plot shows that the Big Sandy feldspars are anomalous; otherwise, the feldspars would have plotted at the high sanidine corner because of their potassic composition and measured a dimension (Wright and Stewart, 1968). The measured a dimension is 8.570-8.591 A, but the a dimension inferred from the $b-c$ plot is about 8.30-8.40 A. Thus, the Big Sandy feldspars have b that is shortened by as much as 0.06 A and c that is shortened by as much as 0.01 A.

Authigenic potassium feldspars with similar anomalous cell dimensions have been reported from tuffs in the Pleistocene Lake Tecopa deposits and tuffs in the Miocene Barstow Formation (Sheppard and Gude, 1965; Martin, 1971). These feldspars also have relatively high boron contents, and Martin (1971) suggested that the anomalies are caused by the partial substitution of boron for aluminum in the feldspar structure. Feldspars of the series $KAlSi_3O_8-KBSi_3O_8$ that were synthesized by Martin (1971) seem to confirm the effect of boron on the cell dimensions.

TABLE 13. — *Unit-cell parameters and boron content of authigenic potassium feldspar*

[Cell parameters were obtained by a least-squares refinement of X-ray powder diffractometer data, utilizing the U.S. Geological Survey's FORTRAN IV Computer Program W9214. The boron content was determined by quantitative spectrographic analysis by J. C. Hamilton on bulk samples of tuff. Locality data are given in table 12]

Parameter or content	1	2	3	4	5	6
<i>a</i> ----- (A) --	8.589±0.003	8.583±0.004	8.578±0.004	8.589±0.002	8.589±0.002	8.573±0.003
<i>b</i> ----- (A) --	12.976±0.003	12.974±0.003	12.976±0.004	12.984±0.002	12.982±0.002	12.986±0.004
<i>c</i> ----- (A) --	7.164±0.001	7.167±0.002	7.170±0.003	7.169±0.002	7.168±0.002	7.167±0.002
β -----	115°59.2'±1.2'	116°0.6'±1.8'	116°3.2'±1.4'	115°59.3'±1.4'	115°55.7'±1.0'	116°1.4'±1.1'
<i>V</i> ----- (A ³) --	717.70±0.23	717.18±0.33	717.57±0.31	718.65±0.23	718.80±0.19	715.91±0.30
Boron --(ppm) --	2,300	1,800	660	2,200	1,500	1,900

QUARTZ

Authigenic quartz is a common constituent in the altered tuffs of the Big Sandy Formation. Quartz is associated with all the other authigenic silicate minerals, as determined by studies of X-ray diffractometer patterns of bulk samples. Studies of the altered tuffs in thin sections, however, have confirmed the association of authigenic quartz with only clay minerals, potassium feldspar, opal, analcime, clinoptilolite, and mordenite. The association of authigenic quartz with analcime and potassium feldspar is especially common. The abundance of quartz in parts of the altered tuffs ranges from trace amounts to about 90 percent.

Quartz occurs either as aggregates of anhedral, nearly equidimensional crystals or as aggregates of fibers. Both varieties occur in irregular, clear patches or they locally line irregular cavities. Individual crystals in the anhedral aggregates are from less than 2 μ m to 80 μ m in diameter and generally have wavy extinction. The fibrous variety is about 10 μ m to 125 μ m long and is either length slow or length fast. Quartz also occurs as spherulites, as much as 250 μ m in diameter. Clusters of mutually interfering spherulites commonly fill irregular cavities (fig. 21). Most of the quartz is chalcedonic, inasmuch as the indices of refraction are below 1.54.

DIAGENETIC FACIES

DISTRIBUTION

Three diagenetic facies can be recognized in the tuffs of the Big Sandy Formation. Tuffs nearest the margin of the formation are characterized by zeolites other than analcime and are herein termed the "nonanalcimic zeolite facies." Tuffs in the central part of the lake basin are characterized by potassium feldspar and are termed the "potassium feldspar facies." Those tuffs intermediate in position between the nonanalcimic zeolite facies and the potassium feldspar facies are characterized by analcime and are termed the "analcime facies." No relict fresh glass was recognized in any of the tuffaceous rocks of the Big Sandy Formation.

The boundaries between the facies are laterally gradational and difficult to recognize in the field. X-ray powder diffractometer data of bulk samples, coupled with thin-section study, are considered essential for positive identification and placement in the proper facies.

A map showing the diagenetic facies for a composite of all the tuffaceous rocks in the Big Sandy Formation is given in figure 22, and a map showing the facies for only the lower marker tuff is given in figure 23. The boundary between the nonanalcimic zeolite facies and the analcime facies was placed at the first appearance of analcime, and the boundary between the analcime facies and the potassium feldspar facies was placed at the first appearance of authigenic potassium feldspar. Most sample localities shown on the maps represent more than one sample (table 14). As many as 25 samples were collected and studied from tuffaceous units at certain localities, and as many as six samples of a single tuff were examined from certain localities. Therefore, each locality shown on the maps does not represent an equal quantity of mineralogical data.

The diagenetic facies in plan are elongated parallel to the depositional basin. The nonanalcimic zeolite facies and the analcime facies are broadest at the northern part of the basin which was the major inlet of the ancient lake. The nonanalcimic zeolite facies is also broad and extends basinward near the other inlets. In a general way, the nonanalcimic zeolite facies and the analcime facies narrow where the basin narrows. About 3 miles southeast of Wikieup, where the basin was narrowest, both the nonanalcimic zeolite and analcime facies are absent along the eastern margin (fig. 22); the potassium feldspar facies is in contact with rocks older than the Big Sandy Formation for a distance of about 0.2 mile. These features suggest that the chemical depositional environment affected, if not controlled, the distribution of the diagenetic facies.

FIELD DESCRIPTION

The altered tuffs of the Big Sandy Formation are generally white to pale gray or pastel shades of yellow, brown, pink, or green with a dull or earthy luster. Most of these tuffs are resistant and form ledges. Original sedimentary structures, such as bedding and ripple marks, are generally preserved in the altered tuffs. Although no relict glass was recognized in any of the tuffaceous rocks, the original vitroclastic texture is commonly preserved, especially in the nonanalcimic zeolite facies. Preservation of these features is convincing evidence that the present differences in composition and mineralogy of the tuffs are due to postdepositional processes.

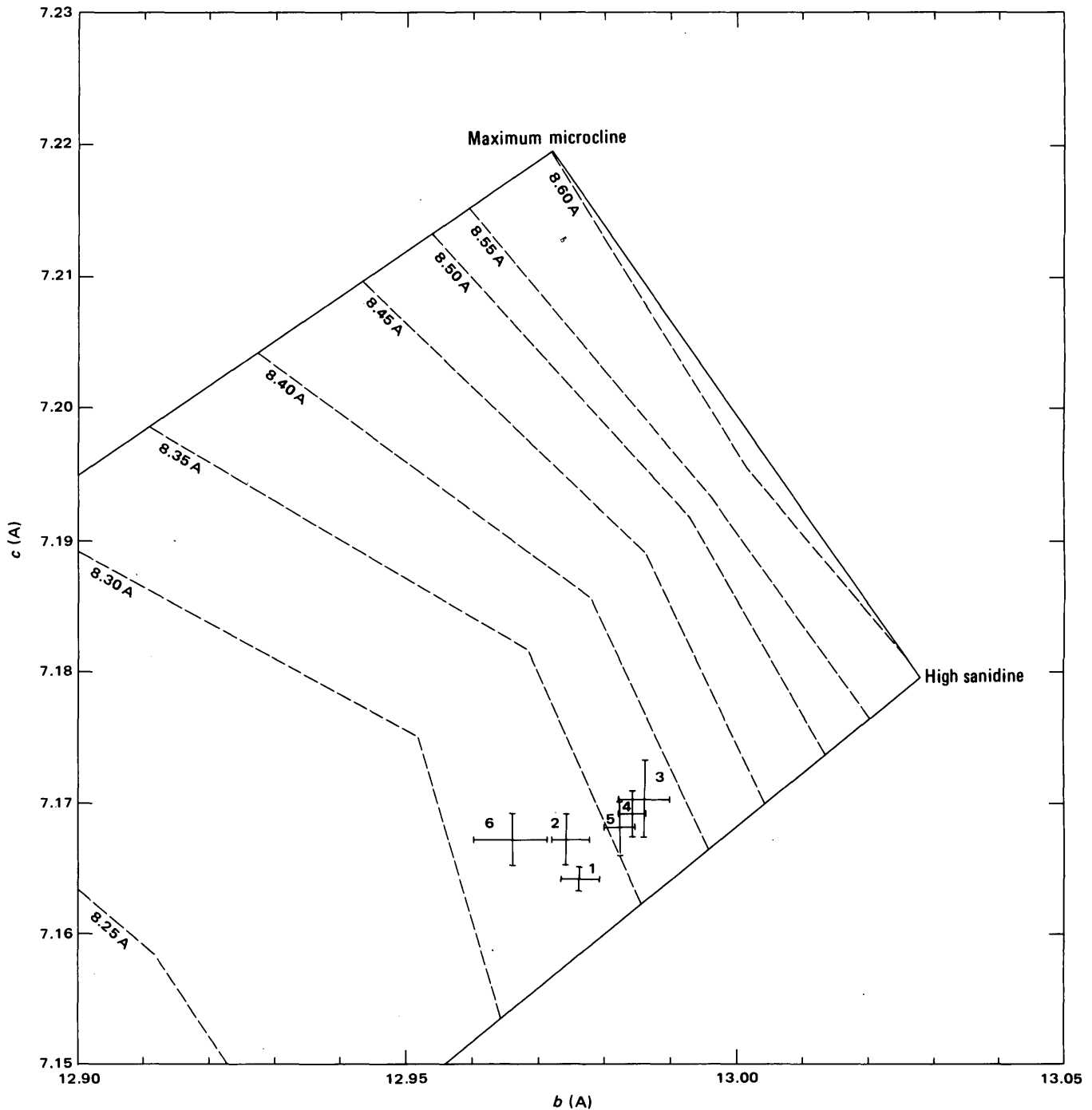


FIGURE 20. — Potassium-rich portion of Wright and Stewart's (1968) b - c quadrilateral for alkali feldspars, which has been contoured for a (dashed lines). The b - c dimensions are plotted for the six specimens given in table 13. Error bars represent plus or minus one standard deviation.

The authigenic silicate minerals in the altered tuffs generally cannot be positively identified in the field because of the very small size of the crystals. Where the altered tuff is nearly monomineralic, certain gross physical properties of the rock may aid field identification. Tuffs of the non-analcimic zeolite facies are generally more resistant and show better preservation of the vitroclastic texture than tuffs of the analcime or potassium feldspar facies. Most

nonanalcimic tuffs break with a platy or subconchoidal to conchoidal fracture (figs. 24–26). Tuffs rich in chabazite are commonly white to pale yellow and break with a platy or subconchoidal fracture (fig. 25). Erionite-rich tuffs are yellow to orange and generally break with a platy fracture (fig. 26). Tuffs rich in clinoptilolite are generally white, gray, or pale yellow and break with a conchoidal fracture. Tuffs rich in other zeolites of the nonanalcimic zeolite facies

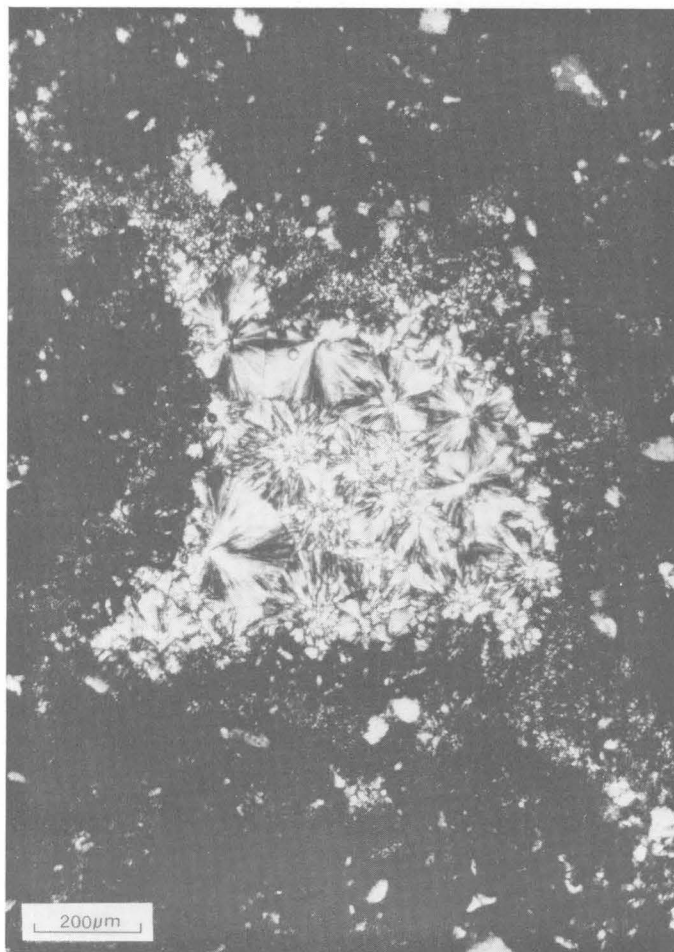


FIGURE 21. — Spherulitic quartz, which has filled an irregular cavity in the lower marker tuff. Much of the dark area of the photomicrograph consists of finely crystalline authigenic potassium feldspar. Crossed nicols.

do not seem to have distinctive megascopic properties that help their identification.

Tuffs that consist mostly of analcime are generally green or greenish yellow and are porous and friable. Their most characteristic features are a sugary texture and the poor preservation or absence of the original vitroclastic texture. The analcime tuffs generally resemble well-sorted siltstone to the unaided eye. However, analcime euhedra are commonly visible with the aid of a hand lens. Analcime tuffs break with an irregular or blocky fracture (fig. 27).

Tuffs altered chiefly to potassium feldspar are generally white or pale yellow, porous, and very friable. If minor or no authigenic quartz is associated with the feldspar, the tuff can easily be crumbled in one's hand. Potassium feldspar-rich tuffs commonly show poor preservation of the original vitroclastic texture and break with an irregular fracture.

PETROGRAPHY

The mineralogy of the tuffaceous rocks was determined by study of X-ray powder diffractometer data of bulk

samples (table 14), supplemented by thin-section study. Thin sections were especially useful for determining age relationships of the authigenic minerals but were generally not examined until the mineralogy of the samples was known by X-ray methods. Optical identification of the zeolites is difficult because of their small crystal size and similar optical properties and morphology.

Crystal fragments, unlike the original vitric materials, are generally unaltered in the tuffaceous rocks. Authigenic potassium feldspar, however, locally replaced plagioclase; and calcite locally replaced detrital and pyrogenic crystal fragments, as well as the authigenic silicate minerals, including analcime and potassium feldspar.

NONANALCIMIC ZEOLITE FACIES

The vitroclastic texture is generally well preserved in tuffs of the nonanalcimic zeolite facies (figs. 28 and 29). Some of the zeolitic tuffs lack the relict texture or have only vague ghosts of shards, where the zeolite is coarsely crystalline or where authigenic clay minerals are absent. Typical pseudomorphs of shards consist of a thin marginal film of montmorillonite, several micrometers thick, succeeded inwardly by crystals of one or more zeolites. The thin montmorillonite film emphasizes the pseudomorphs, especially if a thin section is viewed under crossed nicols (fig. 30). The pseudomorphs may be either solid or hollow, and both types can be recognized in some thin sections. Hollow pseudomorphs seem to have formed from relatively large vitric particles and are generally less abundant than solid ones.

Nearly monomineralic tuffs of chabazite, clinoptilolite, erionite, and phillipsite were recognized in the Big Sandy Formation, but most tuffs consist of two or more zeolites in addition to the nearly ubiquitous authigenic clay minerals. The tuffs consist very commonly of two zeolites, less commonly of three zeolites, and rarely of four zeolites. The following two-, three-, and four-zeolite associations are recognized in the nonanalcimic zeolite facies:

Zeolite Associations

[Ch, chabazite; Cl, clinoptilolite; E, erionite; H, harmotome; M, mordenite; P, phillipsite]

Two zeolites	Three zeolites	Four zeolites
Ch+Cl	Ch+Cl+E	Ch+Cl+E+H
Ch+E	Ch+Cl+P	
Ch+P	Ch+E+P	
Cl+E	Cl+E+P	
Cl+M	Cl+E+H	
Cl+P	Cl+E+M	
E+P		

The most common associations of two zeolites are clinoptilolite plus erionite, followed by clinoptilolite plus phillipsite. The most common associations of three zeolites are chabazite plus clinoptilolite plus erionite, followed by

ZEOLITES AND AUTHIGENIC SILICATE MINERALS, BIG SANDY FORMATION, ARIZONA

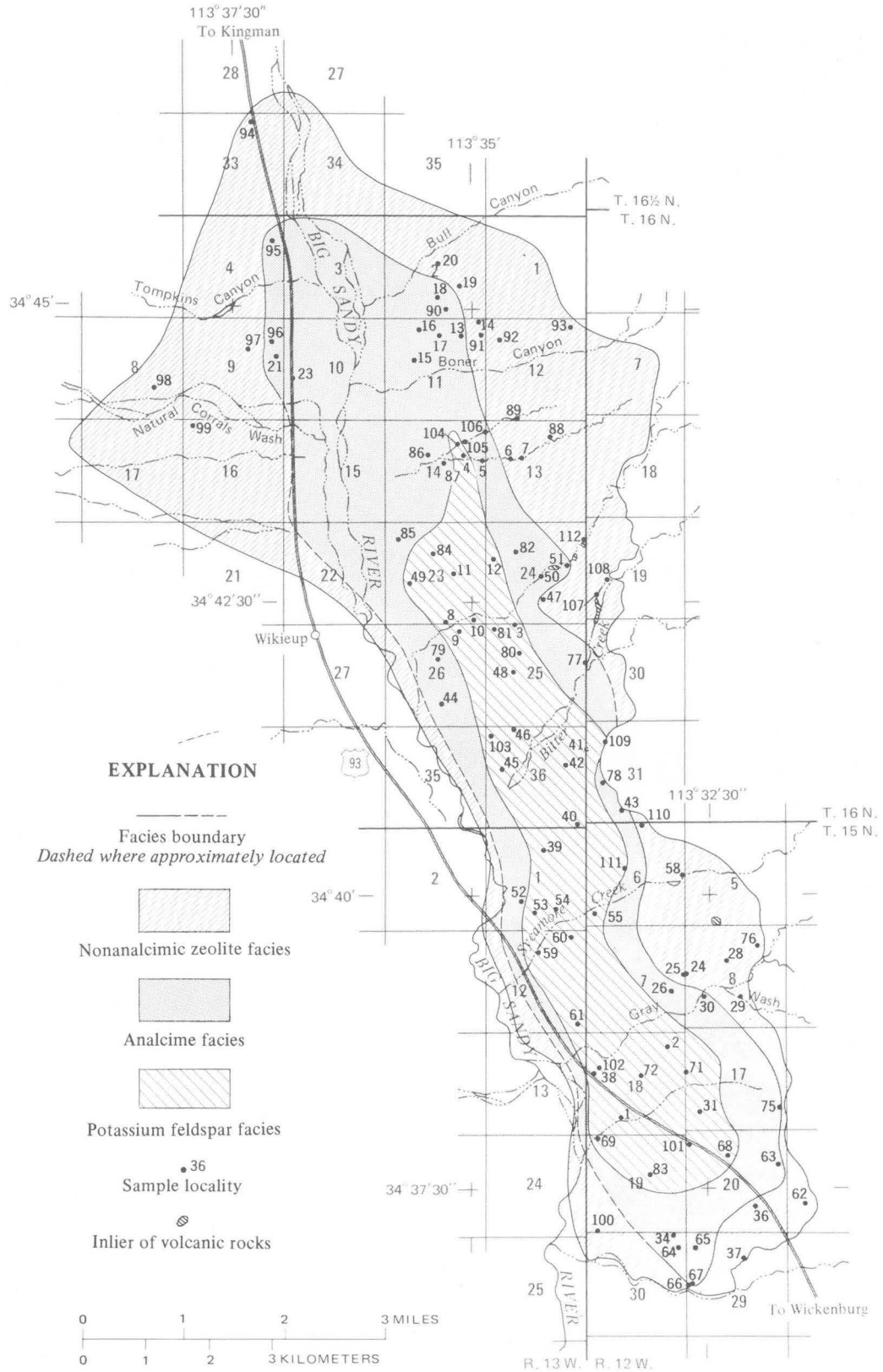


FIGURE 22. — Diagenetic facies for a composite of all the tuffaceous rocks in the Big Sandy Formation. X-ray analysis of samples given in table 14.

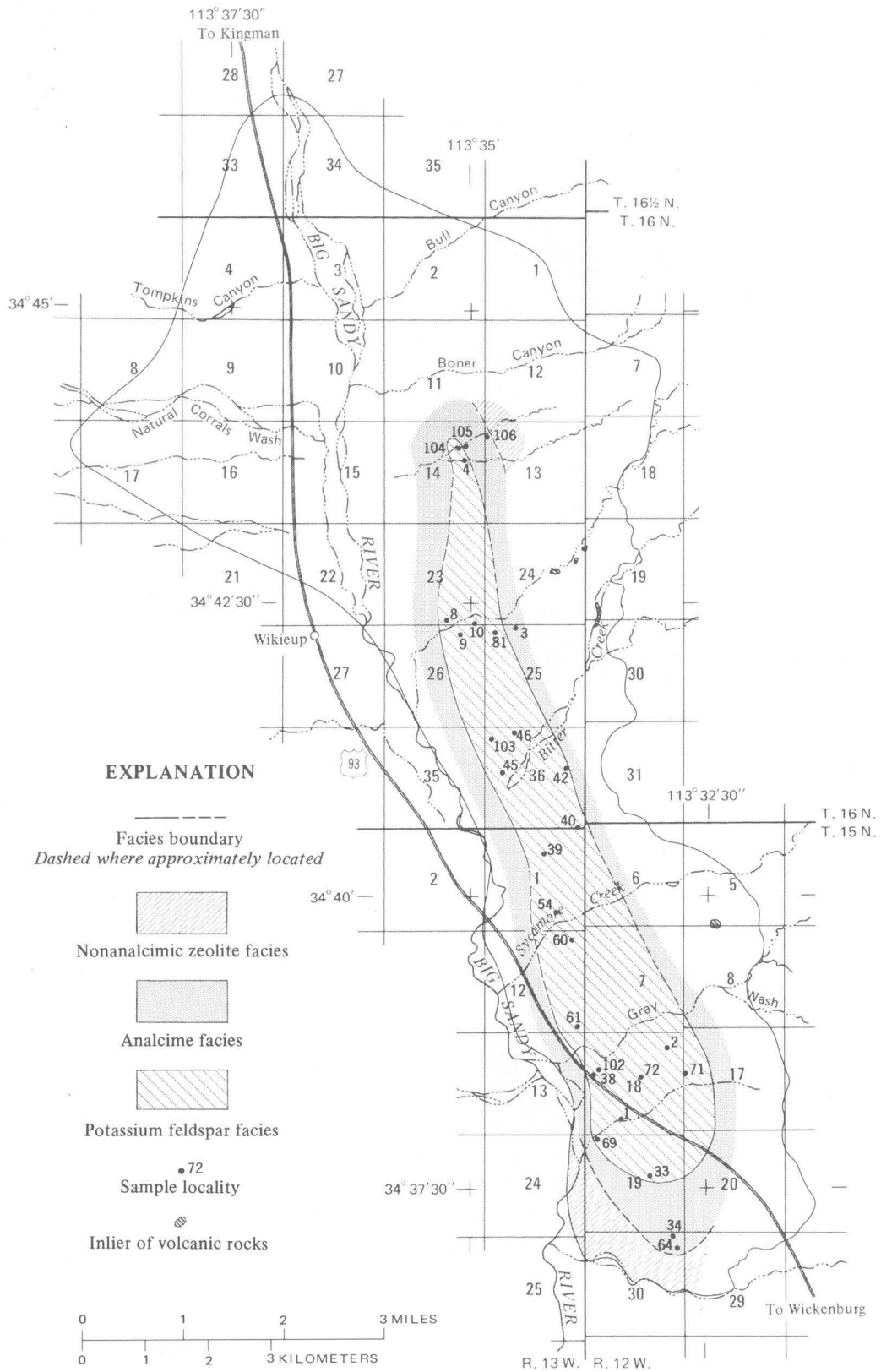


FIGURE 23. — Diagenetic facies for the lower marker tuff of the Big Sandy Formation. X-ray analysis of samples given in table 14.

ZEOLITES AND AUTHIGENIC SILICATE MINERALS, BIG SANDY FORMATION, ARIZONA

TABLE 14. — Mineralogic composition of tuffaceous rocks of the Big Sandy Formation, as estimated from X-ray diffractometer patterns of bulk samples

[— looked for but not found; Tr., trace. Clay 10A: authigenic illite, pyrogenic and detrital albitite, and detrital muscovite. Quartz includes authigenic, pyrogenic, and detrital varieties. Plagioclase and hornblende are pyrogenic and detrital. Other: chiefly dolomite; sample C from Loc. 42 contains a trace of barite; samples B and D from loc. 37 contain a trace of gypsum; and sample SW-2-6 from loc. 2 contains a trace of halite. Sample taken: Tu, upper marker tuff; Tl, lower marker tuff; L, below lower marker tuff, but exact stratigraphic position unknown; M, between lower marker tuff and upper marker tuff but exact stratigraphic position unknown; U, above upper marker tuff but exact stratigraphic position unknown; Ms, mudstone; Ss, sandstone; St, siltstone; T, tufl]

			X-ray analysis (parts of 10)																	
Loc. (fig. 3)	Field No.	Sample text	Clay, 10A	Clay, 14A	Analcime	Chabazite	Cimopitilolite	Erionite	Harmotome	Mordenite	Phillipsite	Potassium feldspar	Opal	Quartz	Calcite	Plagioclase	Hornblende	Other		
1	SW-1-11	3 ft above Tl, Ms	3	1								3			Tr.	3	Tr.			
		10F Tl, 31 in. above base											5		4	Tr.				
		10E Tl, 23 in. above base	1			2							5			2				
		10D Tl, 16 in. above base				6							4							
		10C Tl, 13 in. above base	2			2							2		4	Tr.		Tr.		
		10B Tl, 8 in. above base	1										8			Tr.	1			
		10A Tl, at base	1			2							6			1				
		9 2 ft below Tl, Ms	6										2			Tr.	2			
		8 6 ft below Tl, T	2			1										Tr.	6			
		7 21 ft below Tl, Ms	1	2		1							4			2	Tr.	Tr.		
		6 26 ft below Tl, St	5		Tr.										3	Tr.	2	Tr.		
		5 31 ft below Tl, Ms	3	2	Tr.								4			Tr.	1	Tr.		
		4B 35 ft below Tl, T, at upper part	2		2								6			Tr.				
		4A 35 ft below Tl, T, at lower part	3		3								3			1		Tr.		
		3 38 ft below Tl, Ms	4	Tr.									2			Tr.	4	Tr.		
2B 42 ft below Tl, T, at upper part	2										8			Tr.						
2A 42 ft below Tl, T, at lower part	2										7			1		Tr.				
1 48 ft below Tl, Ms	7										2			1						
2	SW-2-8B	75 ft above Tl, T, at upper part	1									4	7		Tr.					
		8A 75 ft above Tl, T, at lower part	2		4								3	1	Tr.					
		7 62 ft above Tl, Ms	7										2			1		Tr.		
		6 55 ft above Tl, T	2											Tr.	8	Tr.	Tr.	Tr.		
		4 51 ft above Tl, T	2										8			Tr.				
		2 24 ft above Tl, Ms	6										4			Tr.				
		1C Tl, at top	1		1								8							
		1B Tl, 14 in. above base	1										10							
		1A Tl, at base	1										9			Tr.				
		3	SW-3-15B	148 ft above Tu, Ms	3	5												Tr.	2	
				15A 120 ft above Tu, Ms	1												8	Tr.	1	
				14C 108 ft above Tu, Ms	2	2											3	1	2	Tr.
				14B 103 ft above Tu, T	Tr.	2	6								1			Tr.	1	
				14A 99 ft above Tu, T	Tr.		9										1		Tr.	
				13B 94 ft above Tu, T, at upper part	Tr.	7											2		1	
13A 94 ft above Tu, T, at lower part	Tr.			1	7											2				
12D 83 ft above Tu, Ms	4				Tr.											Tr.	6	Tr.		
12C 58 ft above Tu, T, at upper part	3				3								2			Tr.	2			
12B 58 ft above Tu, T, at lower part				Tr.	8								Tr.			2				
12A 48 ft above Tu, T	1				1								4			1	3			
10B 21 ft above Tu, T	1				9								Tr.							
10A 16 ft above Tu, Ms	5				1										2		2			
9C Tu, at top	Tr.				10												Tr.	Tr.		
9B Tu, 2 in. above base	1			4											3	1	1	Tr.		
9A Tu, at base	Tr.		10								Tr.									
8 5 ft below Tu, Ms	2		Tr.										2	Tr.	7					
7 11 ft below Tu, T	1		8								1					Tr.				
5 13 ft above Tl, Ss	1		Tr.										1	Tr.	6	2				
4 12 ft above Tl, T	Tr.		7								1			Tr.	2					
2C Tl, at top	Tr.	Tr.	8										1	Tr.	1					
2B Tl, 9 in. above base	Tr.	Tr.	8											Tr.	2					
2A Tl, at base	Tr.	Tr.	10																	
4	C	1B 3 ft below Tl, Ss	2	1	Tr.									2	Tr.	4	1			
		1A 6 ft below Tl, Ms	3	2	Tr.									3	Tr.	2	Tr.			
		Tl, at upper part	Tr.		9							Tr.			Tr.	1				
5	A	Tl, at lower part	Tr.		9						Tr.				Tr.	1				
		4 ft below Tl, Ms	1		Tr.									5		4				
		U, T, at top	1		6		3										Tr.			
6	B	U, T, 46 in. above base	1											2		2				
		U, T, 35 in. above base	3				Tr.							4	Tr.	3				
		U, T, 22 in. above base	2				Tr.							4	Tr.	4				
7	C	U, T, 12 in. above base	2				2							3		3				
		U, T, at base		2	8															
		U, T, near middle				1	10													
8	A	U, T, at base				10														
		U, Ss	Tr.				3							4		3				
		Tl, at upper part	Tr.		9							1								
9	B	Tl, 5 in. above base	3		3										Tr.					
		Tl, at lower part	2		3										Tr.					
		Tl, at upper part	5		3										Tr.	1				
10	A	Tl, near middle	2		3										Tr.	2				
		Tl, at lower part	Tr.		4							6								
		Tl, at upper part			3							7			Tr.					
11	B	U, T			8															
		U, T	Tr.		8															
		U, T	Tr.		2															
12	A	U, T, at upper part	2	Tr.	1															
		U, T, at lower part	Tr.	1	Tr.										4	6	1	3		
		U, T, at top	Tr.	2	7										1					
12	D	U, T, near middle	Tr.	2	8										Tr.					
		U, T, at base	Tr.	2	8										Tr.					
		U, T	Tr.	2	8										Tr.					

TABLE 14. — Mineralogic composition of tuffaceous rocks of the Big Sandy Formation as estimated from X-ray diffractometer patterns of bulk samples — Continued

Loc. (fig. 3)	Field No.	Sample taken	X-ray analysis (parts of 10)															
			Clay, 10A	Clay, 14A	Analcime	Chabazite	Clinoptilolite	Erionite	Harmotome	Mordenite	Phillipsite	Potassium feldspar	Opal	Quartz	Calcite	Plagioclase	Hornblende	Other
13	SW-13-10B	U, Ms	2	4										2	Tr.	2	Tr.	
		10A U, Ms	4	3										Tr.	3	Tr.	Tr.	
		9 U, Ss	1	2										1	Tr.	5	1	
		8B U, T	Tr.	3	Tr.	Tr.								3	Tr.	2	Tr.	
		8A U, T	Tr.		Tr.						8					2		
		7B U, Ms	2	2											1	3	Tr.	
		7A U, Ms	2	3	Tr.										2	Tr.	2	Tr.
		6 U, Ss	2	3											2	Tr.	3	Tr.
		4B U, T, at top	Tr.			2	5	3							2	Tr.		
		4A U, T, at base				Tr.	1	9										
13	2B	U, T, at upper part	1		7									1		1	Tr.	
		2A U, T, at base	1		6									1	2	Tr.	Tr.	
		1 U, Ms	3	3										2	2	Tr.	Tr.	
14	C B	U, T, at upper part		1		8							1		Tr.			
		U, T, near middle				9		1										
15	A A	U, T, at base		1		9									Tr.	1		
		U, T	Tr.	1	8													
16	C B	U, T	Tr.	1	9													
		A U, T	Tr.	1	9								1	Tr.	Tr.			
17	C B	U, T			10											Tr.		
		A U, T		Tr.	8									2	Tr.	Tr.		
18	A B	U, T	Tr.	10									Tr.		Tr.			
		A U, T	Tr.	1	9										Tr.	Tr.		
19	A B	U, T	Tr.		2			1			2			4				
		A U, T	Tr.	Tr.		10										Tr.		
20	A A	U, T	Tr.	Tr.		9					1							
		A U, T	Tr.	2	4	Tr.	Tr.	4										
21	C B	U, T, at top	2	2	3	1	Tr.	Tr.						1		1		
		B U, T, near middle	Tr.		6	2	Tr.	2								Tr.		
23	A C	U, T, at base	1	Tr.	6	1	Tr.	2	Tr.							Tr.		
		B U, T, at top	1	Tr.	8		Tr.			Tr.				1				
		A U, T, at upper part	Tr.	Tr.	8		1	1	Tr.									
24	A B	U, T, at lower part	Tr.	2	6										1	Tr.		
		A U, T, at upper part					1				1				7	1		
25	B A	U, T, at base					Tr.								7	1		
		A U, T	1							4				4	1			
26	SW-26-10	9A U, T	1	1							7		1			Tr.		
		9B 97 ft above Tu, Ms	2								4			4				
		75 ft above Tu, T, at upper part					10				Tr.			Tr.				
		8 75 ft above Tu, T, at lower part		2		Tr.	Tr.				2	6		Tr.		1		
		6 62 ft above Tu, Ms	1									8						
		5 30 ft above Tu, Ss	1									6	1	2	Tr.			
		4C 4 ft above Tu, Ms	1									4	3	2				
		4B Tu, at top	Tr.								Tr.			1				
		4A Tu, near middle				Tr.		9			Tr.			1	Tr.	Tr.		
		3 Tu, at base			6		Tr.	4							Tr.		1	
28	B A	8 2 ft below Tu, Ms	2	1							6			Tr.				
		6 6 ft below Tu, T	1	1	1							8		Tr.				
		1 10 ft below Tu, Ms	3													4		
		28 B U, T	2	2			2				1			3				
		A U, T	1	Tr.			9											
		29 A U, Ss					3	1		3				3				
		30 C Tu, at top	Tr.				9					Tr.		1			Tr.	
		B Tu, near middle	Tr.		1		9											
		A Tu, at base	Tr.	Tr.	9		1	Tr.				Tr.			Tr.			
		31 A M, T	Tr.		5		Tr.					Tr.		5			Tr.	
33 E TI, at top	Tr.									Tr.		1			Tr.			
34	SW-34-9	D TI, 31 in. above base	Tr.	Tr.	1								9		Tr.			
		C TI, 26 in. above base	Tr.		6								2		2			
		B TI, 13 in. above base	Tr.				10					Tr.						
		F TI, 11 in. above base	Tr.				10					Tr.					Tr.	
		A TI, at base	Tr.		8							2						
		G 2 ft below TI, Ms	2	Tr.								1		7				
		8E 13 ft above Tu, Ss	Tr.		Tr.									4	Tr.	6		
		8D Tu, at top	Tr.					1						9	Tr.	Tr.		
		8C Tu, 24 in. above base	Tr.						3					6		1		
		8B Tu, 18 in. above base	Tr.	2	7											Tr.		
36	C B	8B Tu, 8 in. above base			4													
		8A Tu, at base		3	7										Tr.			
		6 5 ft below Tu, T	Tr.	Tr.	8									1		1		
		5B 18 ft below Tu, Ss	Tr.	2	1									2	Tr.	1		
		5A 21 ft below Tu, Ms	2	2										5	Tr.	1		
		4C TI, at top	1		6		Tr.							1		1	Tr.	
		4B TI, near middle	1	Tr.	7		1	Tr.			Tr.				1	1		
		4D TI, near middle	Tr.		8		1									1	Tr.	
		4E TI, near middle		1	4		4	1									Tr.	
		4A TI, at base		Tr.	9									1		Tr.	Tr.	
37	C B	3 9 ft below TI, Ss	2		2		1						2	Tr.	3	Tr.		
		2B 12 ft below TI, T	Tr.	10										Tr.	Tr.			
		2A 13 ft below TI, Ss	1		2		2				Tr.			3	Tr.	2	Tr.	
		C U, Ss	1				6							3	Tr.	2	Tr.	

TABLE 14. — Mineralogic composition of tuffaceous rocks of the Big Sandy Formation as estimated from X-ray diffractometer patterns of bulk samples — Continued

Loc. (fig. 3)	Field No.	Sample taken	X-ray analysis (parts of 10)															
			Clay, 10A	Clay, 14A	Analcime	Chabazite	Clinoptilolite	Eriomite	Harmotome	Mordenite	Phillipsite	Potassium feldspar	Opal	Quartz	Calcite	Plagioclase	Hornblende	Other
37	A	U, T	1				4	Tr.										
38	A	Tl, at lower part	Tr.		6								2		3			
39	B	Tl, at upper part		Tr.	3		3					4						
40	A	Tl, at lower part	Tr.									10						
	D	Tl, at top											9				Tr.	
	C	Tl, 20 in. above base			1									8				
41	A	Tl, 13 in. above base		Tr.	1													
	B	Tl, 4 in. above base																
42	A	L, T, at upper part			Tr.													
	B	L, T, at lower part																
43	A	Tl, at top	Tr.		Tr.		6										Tr.	
	C	Tl, near middle			Tr.		10						2					
	A	Tl, at base		Tr.	4		2	Tr.					4					
44	E	25 ft below Tl, T, at upper part	Tr.		1		Tr.											
	D	25 ft below Tl, T, at lower part											9					
45	A	U, T	Tr.		9											1		
	D	Tl, at top	Tr.		8					2								
46	A	Tl, 9 in. above base			2							3	5		Tr.			
	B	Tl, 3 in. above base			3							4	3					
	C	Tl, at base			Tr.							10						
47	A	Tl, at top	Tr.									4	2					
	B	Tl, at upper part										7	3					
48	A	Tl, at base										7	3					
	C	Tl, at upper part										7	3					
49	A	U, Ms	6	4			Tr.							Tr.	Tr.	Tr.	4	
	B	U, T, at top	5		Tr.										1			
50	A	U, T, near middle			8							2				Tr.		
	A	U, T, at base	Tr.		6							4				Tr.		
51	A	U, T, at upper part	Tr.	1	7							1			Tr.	Tr.		
	A	U, T, at base	Tr.		5				5									
52	A	U, T	Tr.		10											Tr.		
	A	U, Ms	Tr.	1	Tr.		8	2										
53	A	U, T	Tr.	2														
	G	18 ft above Tl, T, at upper part	1	3									5					
54	F	18 ft above Tl, T, at base	2	2									3	3		Tr.		
	E	Tl, at top	Tr.	Tr.									9			1		
55	D	Tl, 18 in. above base											10					
	C	Tl, 15 in. above base	Tr.										10					
56	B	Tl, 8 in. above base	2	Tr.									8					
	A	Tl, 2 in. above base	1	Tr.									9					
57	A	U, T, at upper part	Tr.					6					4					
	A	U, T, at lower part	Tr.					7					2					
58	A	U, Ss	Tr.					5								3	2	Tr.
	B	M, T, at upper part	1															
59	A	M, T, at lower part	1														1	Tr.
	B	Tl, at upper part											10					
60	A	Tl, at lower part	3										7					
	C	Tl, at upper part	Tr.	Tr.	2								8					
61	A	Tl, 15 in. above base	4										9					
	B	Tl, at base	Tr.	Tr.									6			1	Tr.	
62	A	U, T	Tr.	Tr.				9	1									
	B	U, T, at top	Tr.	Tr.				5									5	Tr.
63	A	U, T, at base	2	3				7										
	D	U, T	1		3										Tr.	2		
64	A	U, T, at upper part	Tr.		2			7										
	C	U, T, near middle	Tr.		2			7	Tr.									
65	A	U, T, at lower part	Tr.	Tr.	3			3	1									
	B	U, T	Tr.		Tr.			7					10					
66	A	Tl, at upper part	Tr.		3													
	D	Tl, at lower part	Tr.		7													
67	A	Tu, at upper part	Tr.		Tr.			2										
	C	Tu, near middle	Tr.	Tr.	4			4	1									
68	B	Tu, at lower part			1													
	A	5 ft below Tu, T			10				9							Tr.		
69	A	23 ft below Tu, Ss	Tr.	Tr.				1						3			6	
	A	104 ft above Tu, Ss	Tr.					Tr.						6			4	
70	9B	98 ft above Tu, Ss	Tr.											9		Tr.	1	
	9A	93 ft above Tu, T						10										
71	7	58 ft above Tu, Ss	Tr.															
	6D	55 ft above Tu, T																
72	6C	40 ft above Tu, T	1															
	6B	36 ft above Tu, Ss	Tr.	2		4		2	2					1				Tr.
73	6A	23 ft above Tu, Ss	Tr.	Tr.										9	Tr.	1	Tr.	
	5B	12 ft above Tu, Ss	1					3	1					3			2	Tr.
74	5A	10 ft above Tu, T	Tr.					8	2									
	4C	Tu, at top	Tr.					8								2	Tr.	
75	4B	Tu, near middle	Tr.					8								2		
	4A	Tu, at base	Tr.					9	1									
76	2	5 ft below Tu, T	Tr.					10										
	B	U, T	1															
77	A	U, T	Tr.		8									6				Tr.
	C	Tl, at top	2															Tr.
78	B	Tl, near middle	Tr.		9			Tr.							Tr.			
	A	Tl, at lower part	Tr.		9									Tr.				
79	F	75 ft above Tl, T	Tr.	3	1									2	4			Tr.
	E	Tl, at top	Tr.											4	6			Tr.
80	D	Tl, 22 in. above base												8	2			
	C	Tl, 18 in. above base			1									9				
81	A	Tl, 11 in. above base												8	2			
	C	Tl, 11 in. above base												8	2			

TABLE 14. — Mineralogic composition of tuffaceous rocks of the Big Sandy Formation as estimated from X-ray diffractometer patterns of bulk samples — Continued

Loc. (fig. 3)	Field No.	Sample taken	X-ray analysis (parts of 10)															
			Clay, 10A	Clay, 14A	Analcime	Chabazite	Climoptilolite	Erionite	Harmotome	Mordenite	Phillipsite	Potassium feldspar	Opal	Quartz	Calcite	Plagioclase	Hornblende	Other
71	B	Tl, 6 in. above base	3	Tr.									7					
	A	Tl, at base	1										8					
	E	Tl, at top	Tr.										10		1			
	D	Tl, 20 in. above base											10					
	C	Tl, 12 in. above base	Tr.										10					
	B	Tl, 11 in. above base	2										8					
	A	Tl, at base	2										8		Tr.			
75	B	U, T		4	2		Tr.				1				3			
	A	U, T	Tr.	Tr.	5		Tr.				5							
	A	U, Ss	Tr.									2	4		3			
76	A	U, T																
	B	U, T		1	4									5				
	A	U, T	2	1									4		2	1		
	B	L, T	Tr.	1	9										Tr.			
78	B																	
	A	L, Ss	Tr.										6	Tr.	4	Tr.		
	A	U, T		4	3		Tr.				1			2				
79	A	U, Ms	2	Tr.										2				
80	A																	
	B	Tl, at upper part	Tr.		10						Tr.							
	A	Tl, at lower part		1	9						Tr.			Tr.				
82	A	U, Ms	3	2										1	4	Tr.		
84	A	U, T	Tr.		6						4							
	A	U, T																
	A	U, Ss	1		Tr.								6		3			
85	A	U, Ms	4	3											3			
86	A	U, Ms	4	3											3			
87	B	U, T, at upper part		5	5								Tr.		Tr.			
	A	U, T, at lower part		3	7													
88	A	U, Ss	Tr.	Tr.									4		4	Tr.		
89	C	U, T, at top		1	9													
	B	U, T, near middle		4	Tr.			Tr.						6				
	A	U, T, at base		Tr.	10													
90	A	U, T	Tr.	Tr.	9													
	A	U, T	Tr.	Tr.			8	2										
	A	U, T	Tr.	Tr.														
	A	U, Ss	Tr.	Tr.									5		5	Tr.		
	A	U, Ss	Tr.	Tr.									4	3	3			
	A	U, Ss	1	3									4	3	2			
94	A	U, Ss	1	3									4	3	2			
95	C	U, T, at top	Tr.				6								4	Tr.		
	B	U, T, near middle	Tr.			9												
	A	U, T, at lower part	1	1		8									Tr.			
	D	U, T, at base	1	Tr.		2							4		3			
96	B	U, T, at upper part	1	Tr.		2							3		1			
	A	U, T, at lower part	1	Tr.		7		3					3					
97	A	U, Ss	1	2									5		2	Tr.		
98	A	U, Ss	1	3									2	4	Tr.			
99	A	U, Ss	1	1									4	2	1			
100	B	L, Ss	2	Tr.									5	4	4			
	A	L, Ms	3	2									4		1			
101	B	U, Ms	2	1									4	1	2			
	A	U, Ms	2	1									4	Tr.	3	Tr.		
102	C	Tl, at top	1	Tr.	4													
	B	Tl, 14 in. above base	Tr.	Tr.	5										Tr.			
	A	Tl, at base	3	Tr.														
103	B	Tl, at upper part	2										4					
	A	Tl, at lower part	2										4					
104	SW-104-9	78 ft above Tl, Ms	3	3		Tr.	Tr.					2	1		4			
	8	60 ft above Tl, Ms	5										1	1	2	5		
	7D	51 ft above Tl, T	3	2	Tr.							5			Tr.			
	7C	50 ft above Tl, T	3	2									2	Tr.	1	2	Tr.	
	7B	48 ft above Tl, T	1	1	Tr.								3		5	Tr.		
	7A	42 ft above Tl, T	2	2	3								3	Tr.	3	Tr.		
	6	38 ft above Tl, Ms	2	1	Tr.								3	Tr.	1	3	Tr.	
	5B	26 ft above Tl, Ss	1	1	Tr.								3	1	2	3	Tr.	
	5A	18 ft above Tl, St	1	1	Tr.								3	2	3	Tr.		
	4	3 ft above Tl, T	Tr.	Tr.	10							Tr.	5	Tr.	3	Tr.		
	3	1 ft above Tl, St	3										3	Tr.	4	Tr.		
	2	Tl	Tr.		9								1					
	1	11 ft below Tl, Ms	2		Tr.								4		4	Tr.		
105	B	Tl	Tr.		10										Tr.			
	A	Tl	2		4	Tr.		4				Tr.						
106	SW-106-7	92 ft above Tl, Ss					3							3	4		Tr.	
	6	89 ft above Tl, T					7							2				
	5F	71 ft above Tl, Ss	2	1			Tr.	1					4	2				
	5E	45 ft above Tl, T	2	2			2	1					2		1			
	5D	42 ft above Tl, T, at upper part				6	Tr.						2		2	Tr.		
	5C	42 ft above Tl, T, at lower part				8	Tr.						2		2	Tr.		
	5B	15 ft above Tl, Ss	1	Tr.		3							3		3	Tr.		
	5A	11 ft above Tl, T				8	1									1		
	4C	Tl, at upper part	1	1	1		2						2		3			
	4B	Tl, near middle	Tr.					10										
	4A	Tl, at lower part	2	2		Tr.	2	1					1		2			
	3	2 ft below Tl, Ss	5	1			Tr.						2		2	Tr.		
	2B	19 ft below Tl, T, at upper part						10								2		
	2A	19 ft below Tl, T, at lower part	1	1			Tr.						2			2	Tr.	
	1	22 ft below Tl, St	2	2			1						3		2			
107	A	U, T	Tr.	1			9								Tr.			
108	C	U, T	1				1	4	2						2			
	B	U, T	Tr.	3		Tr.	3				4							
	A	U, St	1	3									2		4			
109	B	U, T, at upper part			4									2			Tr.	
	A	U, T, at base			2									6				
110	A	U, Ss	Tr.				3	2					2	3				
111	A	U, T	1	Tr.			4								2			
112	A	U, Ss	2	Tr.			1						3		4			



FIGURE 24. — Natural exposure of light-yellow nonanalcmic zeolitic tuff along northeastern tributary to Boner Canyon, about 3.2 miles northeast of Wikieup. Tuff consists of erionite and clinoptilolite and minor amounts of chabazite.



FIGURE 25. — Natural exposure of white chabazite-rich tuff along northeastern tributary to Boner Canyon, about 3.4 miles northeast of Wikieup. Tuff grades upward into brown sandstone.

clinoptilolite plus erionite plus phillipsite. Absence of other seemingly possible zeolite associations in tuffs of the Big Sandy Formation may be, in part, due to our inability to identify small quantities of a constituent by optical or X-ray techniques.

The paragenesis of authigenic silicate minerals in the zeolitic tuffs can be ascertained by studying the sequence of filling of shard cavities, by contrasting the mineralogy of the pseudomorphed shards with the mineralogy of the matrix, and by studying the mineralogy of the relatively late fillings in vugs and along fractures. The mineral in the interior of a pseudomorph presumably formed later than the minerals nearer the periphery of the pseudomorph. Those minerals in the finely crystalline matrix are presumed to have

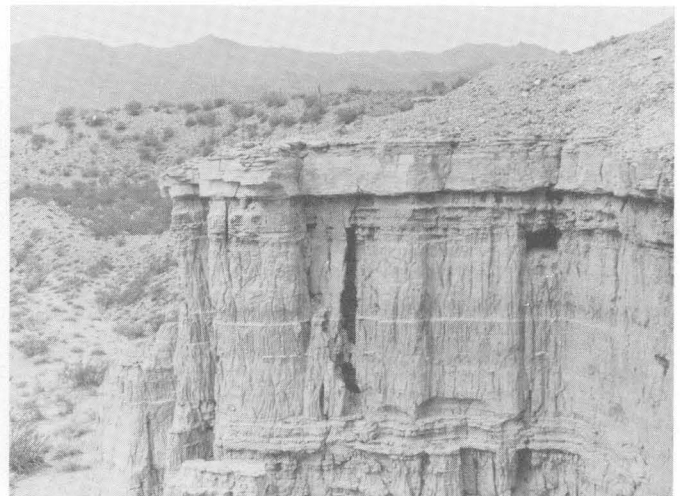


FIGURE 26. — Natural exposure of yellow erionite-rich upper marker tuff along northeastern tributary to Gray Wash, about 5 miles southeast of Wikieup. Tuff is platy, resistant, and 20 inches thick.

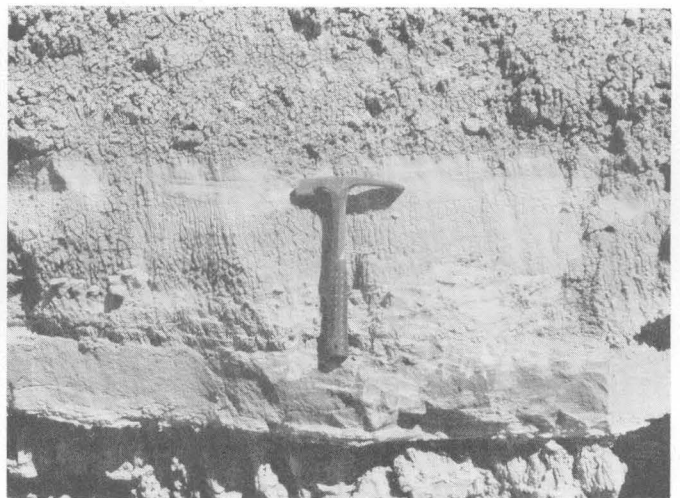


FIGURE 27. — Natural exposure of green analcime-rich lower marker tuff along unnamed tributary to the Big Sandy River, about 2 miles east of Wikieup.

crystallized prior to the minerals that compose the relatively large pseudomorphs. The following sequences of crystallization were determined by using the above criteria:

Paragenesis of authigenic silicate minerals

[Earliest mineral listed on left]

- Montmorillonite-phillipsite-clinoptilolite
- Montmorillonite-harmotome-chabazite
- Montmorillonite-clinoptilolite-quartz
- Montmorillonite-clinoptilolite-erionite
- Montmorillonite-chabazite-clinoptilolite

These relationships indicate that montmorillonite was consistently the earliest mineral to form in the tuffs. Phillipsite, chabazite, and harmotome are relatively early zeolites; and clinoptilolite and erionite are relatively late zeolites. Other age relationships, particularly those concerning mordenite,

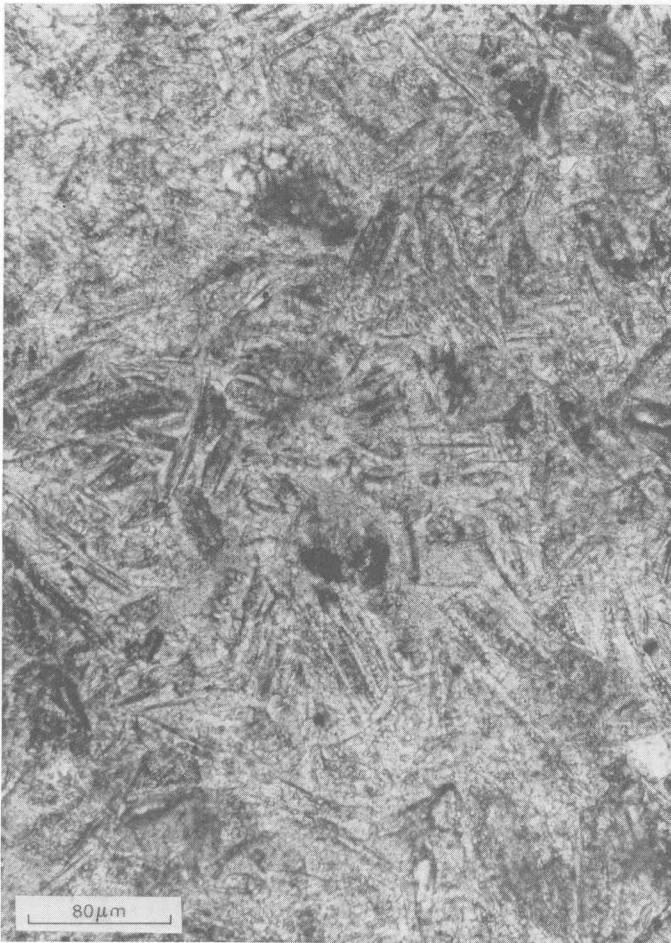


FIGURE 28. — Nonalcalimic zeolitic tuff, showing preservation of vitroclastic texture. Tuff consists of clinoptilolite and a minor amount of erionite. Unpolarized light.

are unknown because the critical textural relations were not recognized in thin sections. Replacement of one zeolite by another was not observed in tuffs of the nonalcalimic zeolite facies, although more than one zeolite commonly occurs in the same sample.

ANALCIME FACIES

Tuffs of the analcime facies characteristically lack evidence of a vitroclastic texture, or they show poor preservation of the texture. Destruction of the vitroclastic texture is especially common in those tuffs that consist entirely of subhedral to euhedral analcime. Some analcime crystals enclose "ghosts" of shards that are outlined by a thin film of montmorillonite.

X-ray diffractometer study has shown that analcime is associated with each of the other zeolites, and thin-section study has shown that analcime replaced each zeolite except mordenite. Analcime may also have replaced mordenite, but mordenite was not recognized in any of the thin sections. Replacement of authigenic montmorillonite by analcime is

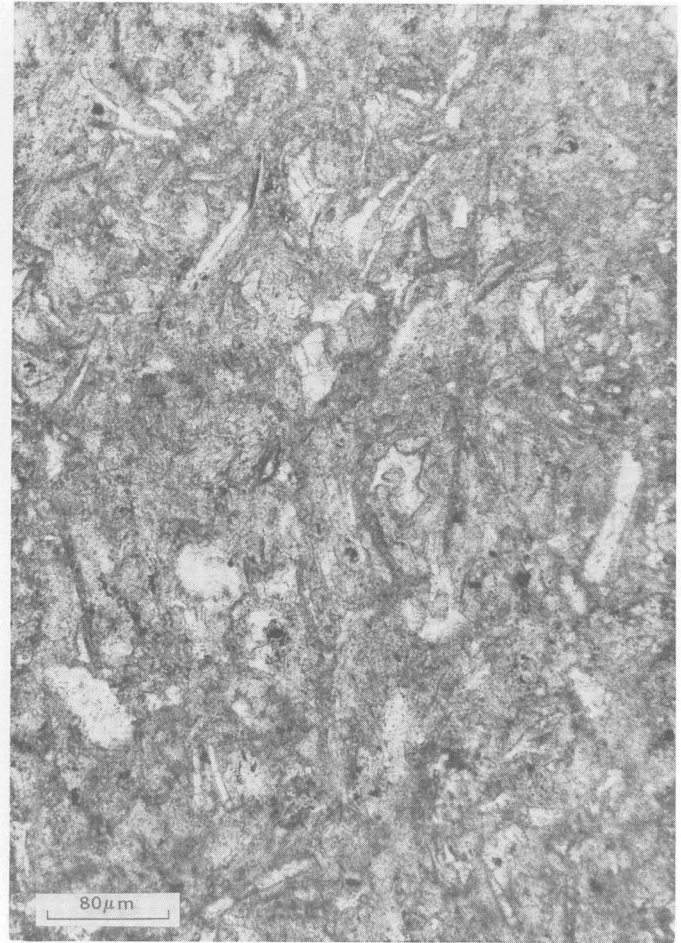


FIGURE 29. — Nonalcalimic zeolitic tuff, showing preservation of vitroclastic texture. Tuff consists of chabazite and a minor amount of clinoptilolite. Unpolarized light.

commonly observed in thin sections. Thus, analcime seems to have formed from preexisting authigenic silicate minerals, chiefly other zeolites. There is no petrographic evidence to suggest that analcime formed directly from the silicic glass shards in the tuffs.

POTASSIUM FELDSPAR FACIES

Tuffs of the potassium feldspar facies are characterized by finely crystalline authigenic potassium feldspar that occurs in trace to major amounts. The potassium feldspar is associated with each of the zeolites except harmotome and mordenite. The association of the authigenic feldspar with analcime is especially common in the Big Sandy Formation. Vitroclastic texture is poorly preserved in tuffs or those parts of tuffs where potassium feldspar is abundant. The vitroclastic texture is recognizable by remnants of clinoptilolite pseudomorphs after shards and by remnants of montmorillonite that vaguely outline shards.

Thin section study of the potassium feldspar-bearing tuffs shows that the feldspar has formed chiefly from precursor

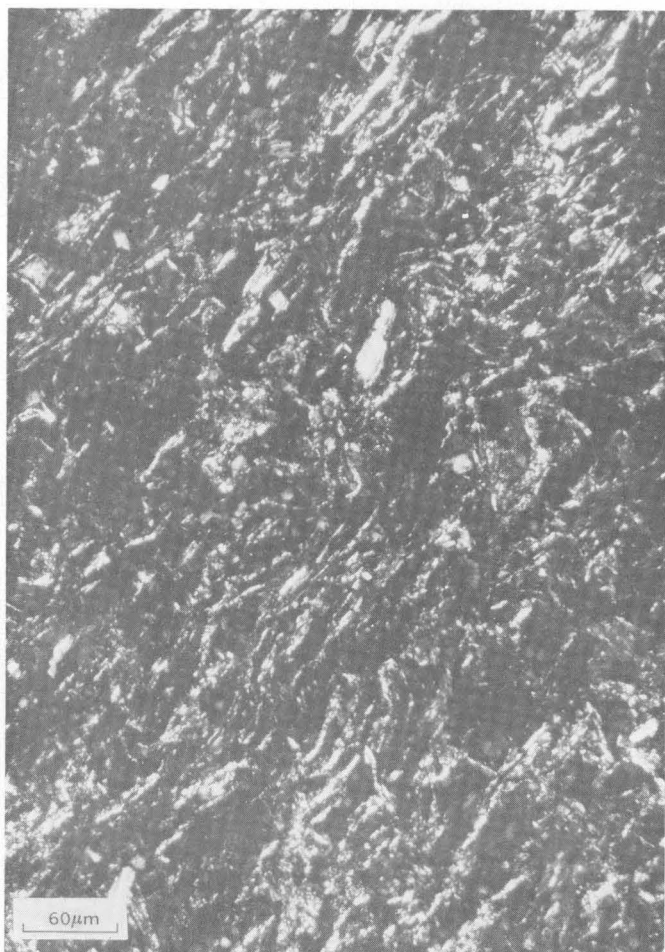


FIGURE 30. — Nonanalcimic zeolitic tuff, showing pseudomorphs of shards that consist of an outer film of montmorillonite (light) and a filling of chabazite and a minor amount of erionite (dark). Crossed nicols.

zeolites. Feldspar replacements of subhedral to euhedral analcime crystals, clinoptilolite pseudomorphs after shards, and phillipsite spherulites were recognized in thin sections. Authigenic potassium feldspar also probably has replaced other associated zeolites, but the textural relations with the other zeolites were not observed in thin sections. Replacement of analcime by potassium feldspar is especially common in the Big Sandy Formation. All stages of the replacement are recognizable, from marginal replacement that commonly gives the analcime crystals a ragged appearance to complete pseudomorphs of finely crystalline potassium feldspar. Where completely replaced by feldspar, the crystal outlines of the analcime precursors are recognizable by clay minerals or irresolvable opaque material.

Authigenic potassium feldspar rarely occurs as replacements of pyrogenic or detrital plagioclase in some of the feldspar-rich tuffs. The replacements are hollow, and some show a boxwork structure similar to that of pseudomorphed plagioclase in tuffs of the Barstow Formation in California (Sheppard and Gude, 1969a, p. 21). All

the replacements consist of untwinned, optically continuous potassium feldspar.

GENESIS OF AUTHIGENIC SILICATE MINERALS

Zeolites of authigenic origin occur in sedimentary rocks that are diverse in lithology, depositional environment, and age throughout the world (Hay, 1966). The zeolites and associated authigenic silicate minerals formed by the reaction of a variety of aluminosilicate materials with interstitial pore water. Silicic volcanic glass, however, is the aluminosilicate material that most commonly served as a precursor for the authigenic zeolites, although clay minerals, feldspars, feldspathoids, and gels have also reacted locally to form zeolites. The zeolites and associated authigenic silicate minerals form during diagenesis by reaction of the volcanic glass with interstitial water, which may have originated either as meteoric water or as connate water of a saline, alkaline lake.

Factors that may control the formation and distribution of zeolites and other authigenic silicate minerals in sedimentary rocks were summarized by Hay (1966) as composition, permeability, and age of the host rock, metastable crystallization, temperature, pressure, and chemistry of the pore water. Inasmuch as nearly all the authigenic silicate minerals in the Big Sandy Formation occur within a given tuff, differences in the composition, permeability, and age of the host rock cannot explain their distribution pattern. The Big Sandy Formation was subjected to only shallow burial; therefore, the temperature and pressure during diagenesis was relatively low. Besides, the difference, if any, in the depth of burial between the nonanalcimic zeolite facies and the potassium feldspar facies was seemingly not great enough to cause the observed pattern. The present authigenic silicate mineralogy of the tuffs and the pattern of distribution of the diagenetic facies probably reflect differences in the chemistry of the pore water during diagenesis.

Experimental work by others indicates that the activity ratio of alkali ions to hydrogen ions and the activity of silica are the major chemical parameters of the pore water that control whether clay minerals, zeolites, or feldspars will form under those conditions approximating surface temperatures and pressures (Hemley, 1959, 1962; Garrels and Christ, 1965, p. 359–370; Hess, 1966). Zeolites and feldspars are favored over clay minerals by relatively high alkali ion to hydrogen ion activity ratios and by relatively high silica activities. The high alkali ion to hydrogen ion activity ratio necessary for the formation of zeolites in a tuff can be attained in the depositional environment of a saline, alkaline lake or in the postdepositional environment by hydrolysis and solution of silicic vitric material by subsurface water. The formation of the authigenic silicate minerals and their distribution pattern in tuffs of the Big Sandy Formation are believed to have been controlled by entrapped saline, alkaline lake water.

**INTERPRETATION OF A SALINE, ALKALINE
DEPOSITIONAL ENVIRONMENT FOR PARTS OF
THE BIG SANDY FORMATION**

The obvious evidence for a saline, alkaline depositional environment — bedded saline minerals — has not been found in the Big Sandy Formation. The chemistry of the water must be inferred from the sedimentary rocks of the formation. Disseminated crystal molds that resemble gaylussite occur in some mudstones and suggest saline conditions during deposition. The molds are most common in mudstones of the potassium feldspar facies, are less common in mudstones of the analcime facies, and are absent in mudstones of the nonanalcimic zeolite facies. The absence of diatomites and unaltered glass in the Big Sandy Formation also suggests that the lake water was at least moderately saline and alkaline. However, the coarse clastic rocks in the marginal parts of the Big Sandy Formation suggest an influx of relatively fresh water, particularly at the northern part of the depositional basin. These rather coarse clastic rocks either lack authigenic zeolites and potassium feldspar or contain zeolites other than analcime.

A saline, alkaline depositional environment for parts of the Big Sandy Formation can be inferred from the occurrence of certain of the authigenic silicate minerals. Such zeolites as clinoptilolite and mordenite occur in either fresh or saline water; however, such zeolites as erionite and phillipsite are found almost exclusively in saline-lake deposits (Hay, 1964, 1966). The occurrence of analcime and potassium feldspar in the tuffs and mudstones suggests a saline, alkaline depositional environment (Sheppard and Gude, 1969a; Surdam and Parker, 1972). The authigenic potassium feldspar in tuffs of the Big Sandy Formation contains anomalously high contents of boron. Studies of boron-bearing authigenic potassium feldspar from several closed-basin deposits suggest that these feldspars are unique to saline, alkaline lacustrine deposits (Sheppard and Gude, 1972b).

**CORRELATION BETWEEN THE WATER CHEMISTRY
OF THE DEPOSITIONAL ENVIRONMENT AND THE
AUTHIGENIC SILICATE MINERALOGY**

Not only was the depositional environment of the Big Sandy Formation a saline, alkaline lake, but there is a strong correlation between the inferred areal variation of the water chemistry and the authigenic silicate minerals in the tuffs. In a general way, the diagenetic facies seem to have resulted from differences in the pH and the salinity of the lake water trapped during deposition of the tuffs. The lake water was probably moderately to highly saline with a pH of at least 9, except near the lake margin where runoff and the ancestral Big Sandy River and its tributaries probably kept the salinity and alkalinity at lower levels. Depending on the influx of fresh water versus the rate of evaporation, this areal chemical zonation of the lake water probably fluctuated during the deposition of the Big Sandy Formation.

The areal distribution of authigenic silicate minerals in the tuffs from zeolites other than analcime to analcime and then to potassium feldspar was due to a chemical zonation of the pore water during diagenesis, and this zonation was probably inherited from the chemical zonation that existed in the lake water during deposition of the tuffs. Those tuffs that contain zeolites other than analcime were deposited in the least saline and alkaline water near the lake margin. Farther basinward, these same tuffs are represented by the analcime and potassium feldspar facies because they were deposited in water of increasing salinity and alkalinity.

Studies of tuffs deposited in young saline lakes where water analyses are available have shown a strong correlation between the water chemistry and the authigenic silicate mineralogy (Hay, 1966; Surdam and Mariner, 1971). Tuffaceous sediments deposited in fresh-water parts of these lakes still contain unaltered glass, but those deposited in saline, alkaline water are altered and contain zeolites, potassium feldspar, or searlesite. Older lacustrine deposits that contain interbedded saline minerals also show a correlation between the inferred salinity of the depositional environment and the authigenic silicate mineralogy of the silicic tuffs. In the Pleistocene deposits of Lake Tecopa, Calif. (Sheppard and Gude, 1968), glass is unaltered in tuff deposited in fresh water; however, the tuffs consist of zeolites where they were deposited in moderately saline water, and of potassium feldspar and searlesite where they were deposited in highly saline water. Tuffs in the Eocene Green River Formation of Wyoming (Iijima and Hay, 1968; Surdam and Parker, 1972) are altered to montmorillonite where they were deposited in fresh water; to clinoptilolite and mordenite, in slightly saline water; to analcime, in moderately saline water; and to potassium feldspar, in highly saline water.

FORMATION OF ZEOLITES FROM SILICIC GLASS

Solution of silicic glass by alkaline and slightly to moderately saline pore water provided the materials necessary for the formation of the zeolites except analcime. The genesis of analcime is discussed in a following section. Deffeyes (1959a) emphasized that zeolites form during diagenesis by solution of the shards and subsequent precipitation of zeolite from the solution, rather than by devitrification of the shards. Mariner and Surdam (1970) suggested that an aluminosilicate gel first precipitates from the solution, and then zeolites grow from the gel. A gel was recently recognized in Holocene tuffs at Teels Marsh, Nev., where the gell is associated with phillipsite (Surdam and Mariner, 1971). Gels or evidence for the previous existence of gels is probably not preserved in ancient zeolitic tuffs; thus, their importance has been overlooked. Laboratory and commercial synthesis of zeolites is commonly accomplished from gels (Zhdanov, 1971).

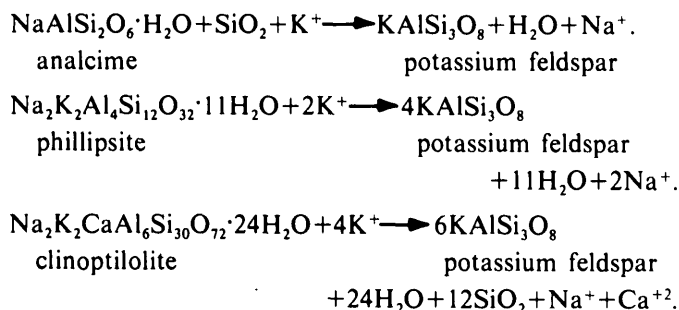
Tuffs in the Big Sandy Formation are commonly interbedded with relatively impermeable mudstones and after

(Sheppard and Gude, 1969a) suggested a correlation between the Si:Al ratio of analcime and the composition of the precursor zeolite. Analcime derived from a siliceous precursor, such as clinoptilolite, has a relatively high Si:Al ratio, whereas, analcime derived from an aluminous precursor zeolite, such as phillipsite, has a relatively low Si:Al ratio. A similar correlation was recognized for analcimes in tuffs of the Big Sandy Formation. Analcime associated with phillipsite, erionite, and clinoptilolite has Si:Al ratios of 2.50–2.58, 2.45–2.60, and 2.58–2.66, respectively. Thus, in a general way, the Si:Al ratio of the precursor zeolite seems to have influenced the Si:Al ratio of analcime. Experimental work by Boles (1971) confirmed this correlation by showing that the Si:Al ratio of analcime synthesized from natural zeolites is chiefly a function of the Si:Al ratio of the zeolite reactants.

REACTION OF ZEOLITES TO FORM POTASSIUM FELDSPAR

Formation of potassium feldspar from zeolite precursors in tuffs that were never deeply buried has been well documented in recent studies. Analcime is replaced by potassium feldspar in tuffs of the Eocene Green River Formation in Wyoming (Iijima and Hay, 1968; Surdam and Parker, 1972). Analcime and clinoptilolite are replaced by potassium feldspar in tuffs of the Miocene Barstow Formation of California (Sheppard and Gude, 1969a). Phillipsite is replaced by potassium feldspar in tuffs of Pleistocene Lake Tecopa, Calif. (Sheppard and Gude, 1968). The formation of potassium feldspar in all of these examples has been correlated with a highly saline and alkaline depositional environment. Petrographic study of the feldspathic tuffs in the Big Sandy Formation has shown that the feldspar replaced analcime, clinoptilolite, and phillipsite. The other zeolites in the tuffs may also have served as precursors for potassium feldspar, but the textural evidence was not observed.

Chemical factors that may affect the formation of potassium feldspar from precursor zeolites are a relatively low activity of H_2O , a relatively high $K^+ : H^+$ ratio, and a relatively high activity of SiO_2 . Simplified representations of the analcime-potassium feldspar, phillipsite-potassium feldspar, and clinoptilolite-potassium feldspar reactions are



The major changes are a gain of potassium and losses of sodium and water. Depending on the composition of the

zeolite, SiO_2 for the reaction may be in excess or deficient in the zeolite precursor.

The increased salinity and alkalinity of the pore water trapped in the tuffs during deposition were probably the major factors responsible for the formation of potassium feldspar. The concentration of potassium was probably higher in the most saline part of the lake basin. Coupled with the high pH, the high potassium concentration would result in a relatively high $K^+ : H^+$ ratio suitable for the crystallization of potassium feldspar. The high pH would also result in increased solubility of SiO_2 and contribute to the stabilization of potassium feldspar (Surdam and Parker, 1972). A relatively high salinity would lower the activity of H_2O and favor the formation of anhydrous potassium feldspar from hydrous zeolites, including analcime.

Silicate reactions are generally regarded as sluggish at low temperatures, but potassium feldspar has been synthesized from a variety of aluminosilicate precursors at temperatures less than $250^\circ C$. Recently, a synthesis of potassium feldspar was accomplished from natural clinoptilolite in a saturated solution of KOH at about $80^\circ C$ after 44 hours (Sheppard and Gude, 1969a). Although this synthetic potassium feldspar was prepared at a higher temperature than that which prevailed during diagenesis of the Big Sandy Formation and was prepared in a chemical environment that probably did not even closely approximate the diagenetic environment, the synthesis does demonstrate the rapidity of the reaction of clinoptilolite to potassium feldspar in a favorable environment.

REFERENCES CITED

- Alietti, Andrea, 1967, Heulanditi e clinoptiloliti: *Mineralog. et Petrog. Acta*, v. 13, p. 119–137 (includes English abs.).
- Baldar, N. A., and Whittig, L. D., 1968, Occurrence and synthesis of soil zeolites: *Soil Sci. Soc. America Proc.*, v. 32, no. 2, p. 235–238.
- Boles, J. R., 1971, Synthesis of analcime from natural heulandite and clinoptilolite: *Am. Mineralogist*, v. 56, nos. 9–10, p. 1724–1734.
- Bradley, W. H., 1928, Zeolite beds in the Green River formation: *Science*, new ser., v. 67, p. 73–74.
- Brobst, D. A., and Tucker, J. D., 1972, Analcime — Its composition and relation to dawsonite in tuff and oil shale in the Green River Formation, Piceance Creek basin, Colorado: *Geol. Soc. America Abs. with Programs*, v. 4, no. 6, p. 369–370.
- Coombs, D. S., and Whetten, J. T., 1967, Composition of analcime from sedimentary and burial metamorphic rocks: *Geol. Soc. America Bull.*, v. 78, no. 2, p. 269–282.
- Deer, W. A., Howie, R. A., and Zussman, J., 1963, Framework silicates, v. 4, *of Rock-forming minerals*: London, Longmans, Green, and Co., 435 p.
- Deffeyes, K. S., 1959a, Zeolites in sedimentary rocks: *Jour. Sed. Petrology*, v. 29, no. 4, p. 602–609.
- , 1959b, Erionite from Cenozoic tuffaceous sediments, central Nevada: *Am. Mineralogist*, v. 44, nos. 5–6, p. 501–509.
- Eakle, A. S., 1898, Erionite, a new zeolite: *Am. Jour. Sci.*, v. 6, no. 4, p. 66–68.
- Garrels, R. M., and Christ, C. L., 1965, *Solutions, minerals, and equilibria*: New York, Harper & Row, 450 p.
- Hay, R. L., 1963, Stratigraphy and zeolitic diagenesis of the John Day Formation of Oregon: *California Univ. Pubs. Geol. Sci.*, v. 42, no. 5, p. 199–262.

- 1964, Phillipsite of saline lakes and soils: *Am. Mineralogist*, v. 49, nos. 9–10, p. 1366–1387.
- 1966, Zeolites and zeolitic reactions in sedimentary rocks: *Geol. Soc. America Spec. Paper* 85, 130 p.
- Hayes, P. T., 1969, Geology and topography, in *Mineral and water resources of Arizona: Arizona Bur. Mines Bull.* 180, p. 35–58.
- Hemley, J. J., 1959, Some mineralogical equilibria in system $K_2O-Al_2O_3-SiO_2-H_2O$: *Am. Jour. Sci.*, v. 257, no. 4, p. 241–270.
- 1962, Alteration studies in the systems $Na_2O-Al_2O_3-SiO_2-H_2O$ and $K_2O-Al_2O_3-SiO_2-H_2O$ in Abstracts for 1961: *Geol. Soc. America Spec. Paper* 68, p. 196.
- Hess, P. C., 1966, Phase equilibria of some minerals in the $K_2O-Na_2O-Al_2O_3-SiO_2-H_2O$ system at 25°C and 1 atmosphere: *Am. Jour. Sci.*, v. 264, no. 4, p. 289–309.
- Hey, M. H., and Bannister, F. A., 1934, Studies on the zeolites; Pt. 7, "Clinoptilolite," a silica-rich variety of heulandite: *Mineralog. Mag.*, v. 23, no. 145, p. 556–559.
- Iijima, Azuma, and Hay, R. L., 1968, Analcime composition in the Green River Formation of Wyoming: *Am. Mineralogist*, v. 53, nos. 1–2, p. 184–200.
- Kirov, G. N., 1965, Calcium-rich clinoptilolite from the eastern Rhodopes: *Sofia University. Annuaire, Fac. Geologie et Geographie*, v. 60, p. 193–200.
- Lee, W. T., 1908, Geologic reconnaissance of a part of western Arizona: *U.S. Geol. Survey Bull.* 352, 96 p.
- Mariner, R. H., and Surdam, R. C., 1970, Alkalinity and formation of zeolites in saline alkaline lakes: *Science*, v. 170, p. 977–980.
- Martin, R. F., 1971, Disordered authigenic feldspars of the series $KAlSi_3O_8-KBSi_3O_8$ from southern California: *Am. Mineralogist*, v. 56, nos. 1–2, 281–291.
- Mason, Brian, and Sand, L. B., 1960, Clinoptilolite from Patagonia, the relationship between clinoptilolite and heulandite: *Am. Mineralogist*, v. 45, nos. 3–4, p. 341–350.
- Morgenstein, Maury, 1967, Authigenic cementation of scoriaceous deep-sea sediments west of the Society Ridge, South Pacific: *Sedimentology*, v. 9, p. 105–118.
- Morrison, R. B., 1940, Ground-water resources of the Big Sandy Valley, Mohave County, Arizona: *Arizona State Water Commissioner*, 6 p.
- Mumpton, F. A., 1960, Clinoptilolite redefined: *Am. Mineralogist*, v. 45, nos. 3–4, p. 351–369.
- Murray, John, and Renard, A. F., 1891, Report on deep-sea deposits, in Report on the scientific results of the voyage of H.M.S. *Challenger* during the years 1873–76: London, 520 p.
- Passaglia, Elio, 1970, The crystal chemistry of chabazites: *Am. Mineralogist*, v. 55, nos. 7–8, p. 1278–1301.
- Pettijohn, F. J., 1957, *Sedimentary rocks* [2d ed.]: New York, Harper & Bros., 718 p.
- Pirsson, L. V., 1890, On mordenite: *Am. Jour. Sci.*, 3d ser., v. 40, p. 232–237.
- Regnier, Jerome, 1960, Cenozoic geology in the vicinity of Carlin, Nevada: *Geol. Soc. America Bull.*, v. 71, no. 8, p. 1189–1210.
- Ross, C. S., 1928, Sedimentary analcite: *Am. Mineralogist*, v. 13, no. 5, p. 195–197.
- 1941, Sedimentary analcite: *Am. Mineralogist*, v. 26, no. 10, p. 627–629.
- Saha, Prasenjit, 1959, Geochemical and X-ray investigation of natural and synthetic analcites: *Am. Mineralogist*, v. 44, nos. 3–4, p. 300–313.
- 1961, The system $NaAlSi_3O_8$ (nepheline)– $NaAlSi_3O_8$ (albite)– H_2O : *Am. Mineralogist*, v. 46, nos. 7–8, p. 859–884.
- Schaller, W. T., 1932, The mordenite-ptilolite group — Clinoptilolite, a new species: *Am. Mineralogist*, v. 17, no. 4, p. 128–134.
- Schoen, Robert, and Lee, D. E., 1964, Successful separation of silt-size minerals in heavy liquids, in *Geological Survey Research 1964: U.S. Geol. Survey Prof. Paper* 501–B, p. B154–859.
- Senderov, E. E., 1963, Crystallization of mordenite under hydrothermal conditions: *Geochemistry*, no. 9, p. 848–859.
- Shaw, D. M., 1956, Major elements and general geochemistry, Pt. 3 of *Geochemistry of pelitic rocks: Geol. Soc. America Bull.*, v. 67, no. 7, p. 919–934.
- Shepard, A. O., 1961, A heulandite-like mineral associated with clinoptilolite in tuffs of Oak Spring Formation, Nevada Test Site, Nye County, Nevada, in *Short papers in the geologic and hydrologic sciences: U.S. Geol. Survey Prof. Paper* 424–C, p. C320–C323.
- Sheppard, R. A., 1969, Zeolites, in *Mineral and water resources of Arizona: Arizona Bur. Mines Bull.* 180, p. 464–467.
- 1971a, Zeolites in sedimentary deposits of the United States — A review, in *Gould, R. F., ed., Molecular sieve zeolites — I: Am. Chem. Soc., Advances in chemistry ser.* 101, p. 279–310.
- 1971b, Clinoptilolite of possible economic value in sedimentary deposits of the conterminous United States: *U.S. Geol. Survey Bull.* 1332–B, 15 p.
- Sheppard, R. A., and Gude, A. J., 3d, 1965, Potash feldspar of possible economic value in the Barstow Formation, San Bernardino County, California: *U.S. Geol. Survey Circ.* 500, 7 p.
- 1968, Distribution and genesis of authigenic silicate minerals in tuffs of Pleistocene Lake Tecopa, Inyo County, California: *U.S. Geol. Survey Prof. Paper* 597, 38 p.
- 1969a, Diagenesis of tuffs in the Barstow Formation, Mud Hills, San Bernardino County, California: *U.S. Geol. Survey Prof. Paper* 634, 35 p.
- 1969b, Chemical composition and physical properties of the related zeolites offretite and erionite: *Am. Mineralogist*, v. 54, nos. 5–6, p. 875–886.
- 1970, Calcic siliceous chabazite from the John Day Formation, Grant County, Oregon, in *Geological Survey research 1970: U.S. Geol. Survey Prof. Paper* 700–D, p. D176–D180.
- 1971, Sodic harmotome in lacustrine Pliocene tuffs near Wikieup, Mohave County, Arizona, in *Geological Survey research 1971: U.S. Geol. Survey Prof. Paper* 750–D, p. D50–D55.
- 1972a, Big Sandy Formation near Wikieup, Mohave County, Arizona: *U.S. Geol. Survey Bull.* 1354–C, 10 p.
- 1972b, Boron in authigenic silicate minerals of closed-basin deposits: *Geol. Soc. America Abs. with Programs*, v. 4, no. 6, p. 410.
- Sheppard, R. A., Gude, A. J., 3d, and Griffin, J. J., 1970, Chemical composition and physical properties of phillipsite from the Pacific and Indian Oceans: *Am. Mineralogist*, v. 55, nos. 11–12, p. 2053–2062.
- Surdam, R. C., and Mariner, R. H., 1971, The genesis of phillipsite in Recent tuffs at Teels Marsh, Nevada: *Geol. Soc. America Abs. with Programs*, v. 3, no. 7, p. 725.
- Surdam, R. C., and Parker, R. D., 1972, Authigenic aluminosilicate minerals in the tuffaceous rocks of the Green River Formation, Wyoming: *Geol. Soc. America Bull.*, v. 83, no. 3, p. 689–700.
- Turekian, K. K., and Wedepohl, K. H., 1961, Distribution of the elements in some major units of the Earth's crust: *Geol. Soc. America Bull.*, v. 72, no. 2, p. 175–192.
- Van Houten, F. B., 1965, Composition of Triassic Lockatong and associated formations of Newark Group, central New Jersey and adjacent Pennsylvania: *Am. Jour. Sci.*, v. 263, p. 825–863.
- Wright, T. L., and Stewart, D. B., 1968, Determination of composition and structural state from refined unit-cell parameters and 2V, Pt. 1 of X-ray and optical study of alkali feldspar: *Am. Mineralogist*, v. 53, nos. 1–2, p. 38–87.
- Zhdanov, S. P., 1971, Some problems of zeolite crystallization, in *Gould, R. F., ed., Molecular sieve zeolites — I: Am. Chem. Soc., Advances in chemistry ser.* 101, p. 20–43.